Role of neoplastic monocyte-derived fibrocytes in primary myelofibrosis

Srdan Verstovsek,[1] Taghi Manshouri,[1] Darrell Pilling,[4] Carlos E. Bueso-Ramos,[2] Kate J. Newberry,[1] Sanja Prijic,[1] Liza Knez,[1] Ksenija Bozinovic,[1] David M. Harris,[1] Erika L. Spaeth,[1] Sean M. Post,[1] Asha S. Multani,[3] Raajit K. Rampal,[5] Jihae Ahn,[6] Ross L. Levine,[5] Chad J. Creighton,[7] Hagop M. Kantarjian,[1] and Zeev Estrov[1]

[1]Department of Leukemia, [2]Department of Hematopathology, and [3]Department of Genetics, University of Texas MD Anderson Cancer Center, Houston, TX 77030
[4]Department of Biology, Texas A&M University, College Station, TX 77433
[5]Leukemia Service, Department of Medicine, Memorial Sloan Kettering Cancer Center, New York, NY 10065
[6]Human Oncology and Pathogenesis Program, Gerstner Sloan Kettering School of Biomedical Sciences, New York, NY 10065
[7]Division of Biostatistics, Dan L. Duncan Cancer Center, Baylor College of Medicine, Houston, TX 77030

Primary myelofibrosis (PMF) is a fatal neoplastic disease characterized by clonal myeloproliferation and progressive bone marrow (BM) fibrosis thought to be induced by mesenchymal stromal cells stimulated by overproduced growth factors. However, tissue fibrosis in other diseases is associated with monocyte-derived fibrocytes. Therefore, we sought to determine whether fibrocytes play a role in the induction of BM fibrosis in PMF. In this study, we show that BM from patients with PMF harbors an abundance of clonal, neoplastic collagen- and fibronectin-producing fibrocytes. Immunodeficient mice transplanted with myelofibrosis patients' BM cells developed a lethal myelofibrosis-like phenotype. Treatment of the xenograft mice with the fibrocyte inhibitor serum amyloid P (SAP; pentraxin-2) significantly prolonged survival and slowed the development of BM fibrosis. Collectively, our data suggest that neoplastic fibrocytes contribute to the induction of BM fibrosis in PMF, and inhibiting fibrocyte differentiation with SAP may interfere with this process.

The Journal of Experimental Medicine

INTRODUCTION

Primary myelofibrosis (PMF) is a myeloproliferative neoplasm characterized by increased BM cellularity, increased numbers of atypical megakaryocytes, decreased erythropoiesis, and extramedullary hematopoiesis (International Agency for Research on Cancer and World Health Organization, 2008). A defining feature of PMF is progressive BM fibrosis, and higher-grade BM fibrosis is associated with poor prognosis (Thiele and Kvasnicka, 2006; Vener et al., 2008). Although constitutive activation of the JAK–STAT pathway plays a key role in the disease pathogenesis (Rampal et al., 2014), treatment of patients with JAK inhibitors such as ruxolitinib usually does not reverse BM fibrosis or eradicate the disease (Harrison et al., 2012; Verstovsek et al., 2012). Therefore, targeting genes or pathways involved in the induction of fibrosis in PMF may be necessary to significantly modify the disease course. However, the mechanism of and the primary cell responsible for BM fibrosis in PMF remain unclear. Because mesenchymal stromal cells (MSCs) produce collagen and fibronectin and cultured PMF BM MSCs do not originate from the neoplastic clone (Jacobson et al., 1978; Nowell and Finan, 1978; Castro-Malaspina et al., 1982; Greenberg et al., 1987; Wang et al., 1992), BM fibrosis in PMF is thought to be reactive, caused indirectly by an overproduction of growth factors by clonal megakaryocytes or platelets that stimulate MSCs to induce BM fibrosis (Groopman, 1980).

However, in other diseases with evolving tissue fibrosis, such as pulmonary fibrosis (Mehrad and Strieter, 2012), end-stage liver or kidney disease (Kisseleva et al., 2006; Reich et al., 2013), heart disease (Keeley et al., 2011), and autoimmune disorders (Reilkoff et al., 2011), fibrocytes, spindle-shaped fibroblast-like cells that differentiate from a subpopulation of $CD14^+$ monocytes (Bucala et al., 1994; Abe et al., 2001; Yang et al., 2002; Pilling et al., 2003; Reilkoff et al., 2011), are associated with the induction of fibrosis. Fibrocytes express markers of both hematopoietic cells (CD34, CD43, CD45, CD68, LSP-1, and major histocompatibility complex class II) and stromal cells (collagen I, collagen III, and fibronectin; Bucala et al., 1994; Abe et al., 2001; Pilling et al., 2009). They also express a variety of chemokine receptors, secrete growth factors and cytokines, regulate tissue repair (Bucala et al., 1994; Reilkoff et al., 2011), and are thought to constitute a subset of myeloid-derived suppressor cells (Zhang et al., 2013). Although they make up <1% of BM cells, fibrocytes

Correspondence to Zeev Estrov: zestrov@mdanderson.org

Abbreviations used: BFU-E, erythroid burst-forming unit; CRP, C-reactive protein; FISH, fluorescence in situ hybridization; GM, granulocyte–macrophage; H&E, hematoxylin and eosin; HPF, high-power field; MSC, mesenchymal stromal cell; NSG, NOD-SCIDγ; PB, peripheral blood; PMF, primary myelofibrosis; SAP, serum amyloid P; SSC, saline-sodium citrate; WBC, white blood cell.

The Rockefeller University Press $30.00
J. Exp. Med. 2016 Vol. 213 No. 9 1723–1740
www.jem.org/cgi/doi/10.1084/jem.20160283

and/or their precursors migrate through the blood to the site of organ damage and participate in induction of fibrosis in the skin, lung, kidney, liver, and heart (Reilkoff et al., 2011). Notably, the differentiation of monocytes into fibrocytes is inhibited by the pentraxin protein serum amyloid P (SAP) component (pentraxin-2), a 125-kD protein produced by the liver (Steel and Whitehead, 1994; Hutchinson et al., 2000), repeated injections of which have been shown to ameliorate fibrosis in multiple organ systems (Haudek et al., 2006, 2008; Pilling et al., 2007; Castaño et al., 2009; Reilkoff et al., 2011).

Because PMF is characterized by increased myeloid proliferation and monocyte-derived fibrocytes have been associated with fibrosis in various organs, we hypothesized that clonal neoplastic fibrocytes play a role in the induction of BM fibrosis in PMF. In this study, we show that the BM of PMF patients harbors more neoplastic functionally distinct fibrocytes and fewer MSCs than hematologically normal BM. In addition, we detected an overabundance of fibrocytes in the BM and spleen of an established PMF mouse model and a xenograft mouse model of PMF created using BM-derived low-density cells from patients with PMF. Treatment of PMF xenograft mice with recombinant human SAP (PRM-151) significantly extended survival and slowed BM fibrosis.

RESULTS

Neoplastic fibrocytes are overrepresented in the BM of patients with PMF and are functionally distinct

To determine whether neoplastic fibrocytes are present in the BM of patients with PMF, we analyzed BM biopsy specimens by immunofluorescence. In PMF BM, we detected very few cells staining positive for CD90 (usually detected in MSCs) and an abundance of cells costaining positive for CD45/CD68 and CD45/procollagen I, markers that are indicative of fibrocytes, but not CD45/PM-2K, a marker of macrophages (Fig. 1 A, top; Pilling et al., 2009). In contrast, hematologically normal BM contained very few cells coexpressing CD45/procollagen I or CD45/CD68, indicating that unlike macrophages and MSCs, fibrocytes were either not present or there were too few to be detected (Fig. 1 A, bottom). Quantitation by multispectral imaging showed significantly more $CD45^+/CD68^+$ and $CD45^+$/procollagen I^+ cells and significantly fewer $CD45^+/PM\text{-}2K^+$ cells (macrophages) and $CD90^+/CD45^-$ (MSCs) in PMF than normal BM (Fig. 1 B). The $CD45^+/CD68^+$ cells had a 20q deletion as the original BM cytogenetic abnormality (Fig. 1 C). Cultured fibrocytes and MSCs from PMF and normal BM had an immunophenotype similar to that of biopsy samples (Fig. 2 A). Morphologically, cultured fibrocytes from PMF BM were characterized by thicker, more convoluted cytoplasmic extensions and more intense staining for type III collagen than those from normal BM, whereas MSCs from normal and PMF BM were not different (Fig. 2, B and C).

Fluorescence in situ hybridization (FISH) analysis of BM smears from a PMF patient with a 20q deletion showed cells with the 20q deletion coexpressing CD45/CD68 (Fig. 1 C) and CD45 and collagen III (Fig. 3 A), suggesting that these neoplastic cells are fibrocytes. To confirm that PMF fibrocytes originate from the neoplastic clone, quantitative allele-specific PCR was used. The JAK2-V617F mutation was detected in cultured fibrocytes, low-density BM cells, granulocytes, and $CD14^+$ and $CD14^-$ leukocytes but not MSCs from 12 patients with JAK2-V617F–postive PMF (Fig. 3 B). Similarly, CALR mutations were detected in low-density BM cells, $CD14^+$ cells, and fibrocytes but not MSCs from seven patients with a CALR mutation (Fig. 3 C). Additionally, cultured fibrocytes from four patients also harbored the chromosomal abnormalities detected in the original BM aspirates (trisomy 1 and the 20q deletion), whereas MSCs did not (Fig. 3 D). Collectively, these data show that BM from PMF patients contains an overabundance of hematopoietic lineage–derived cells that produce procollagen I and fewer MSCs and macrophages than normal BM, and PMF BM–derived fibrocytes originate from the neoplastic clone.

To determine whether PMF fibrocytes were functionally different from normal fibrocytes, we studied the fibrocytes' function. We found that PMF fibrocytes stimulated hematopoietic colony proliferation significantly more than normal fibrocytes (Fig. 4 A), and this effect required cell to cell contact. PMF and normal fibrocytes also showed differential expression of genes known to be deregulated in PMF (Fig. 4 B), and PMF fibrocytes secreted significantly higher levels of inflammatory cytokines/chemokines (Fig. 4 C). Levels of secreted TGF-β from PMF fibrocytes were not different from those of normal fibrocytes (Fig. 4 D). Collectively, these data suggest that PMF fibrocytes are functionally different from normal fibrocytes.

SAP (PRM-151) but not ruxolitinib inhibits PMF and normal BM–derived fibrocytes in vitro

Because our data suggested that fibrocytes play a role in the induction of BM fibrosis in PMF, we looked for a means of inhibiting fibrocyte differentiation. Because levels of SAP, an inhibitor of fibrocyte differentiation, are reduced in patients with fibrotic diseases likely because of increased consumption (Castaño et al., 2009; Murray et al., 2011), we measured SAP in plasma samples from 39 patients with PMF and nine healthy age-matched individuals. Plasma SAP levels were significantly lower in PMF patients than in normal donors (Fig. 5 A). In contrast, levels of C-reactive protein (CRP) were higher in PMF patients than in normal donors (Fig. 5 B). Albumin levels were the same in both groups (Fig. 5 C).

In culture, PMF BM–derived fibrocyte differentiation was significantly inhibited by SAP (PRM-151) in a dose-dependent manner. However, PMF fibrocytes were less sensitive to SAP than were normal BM–derived fibrocytes (Fig. 5, D and E). In contrast, the JAK2 inhibitor ruxolitinib had no significant effect on fibrocyte differentiation (Fig. 5 F).

Fibrocytes are expanded in BM and spleen of MPL-W515L mice

To determine whether, like in human PMF BM, fibrocytes are increased in a PMF mouse model, we analyzed BM and

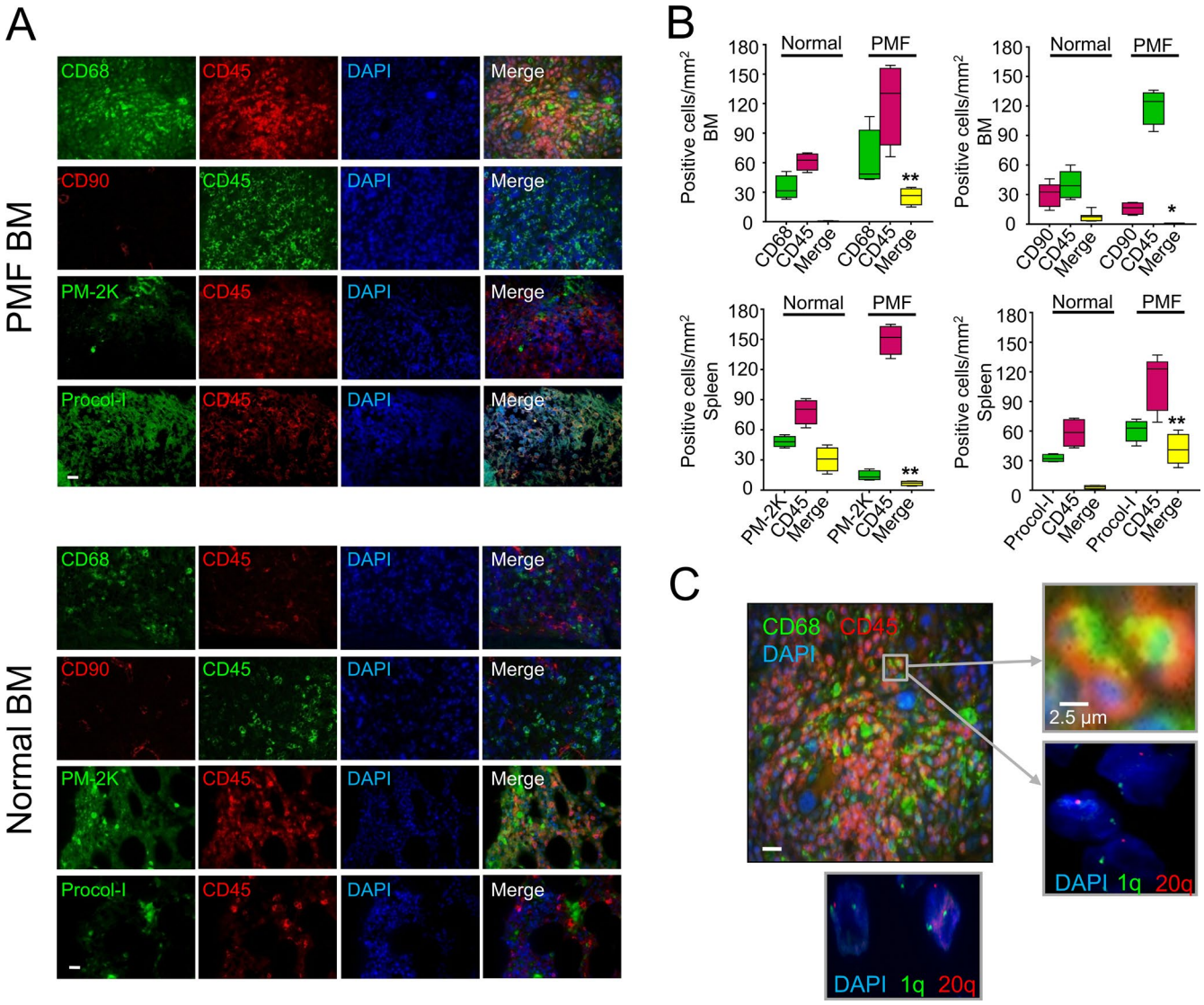

Figure 1. **Detection of neoplastic fibrocytes in PMF BM biopsy specimens.** (A) Immunofluorescent staining of BM biopsy sections from three PMF patients (top) or three normal controls (bottom). Staining for CD45 and CD68 was used to discriminate monocyte-derived cells ($CD45^+/CD68^+$) from CD68-positive MSCs. CD45 and procollagen I (Procol-I) were used to detect fibrocytes. CD90 was used to detect MSCs that do not express CD45, and CD45 and PM-2K were used to detect tissue macrophages. Images are representative of three patients. Bars, 50 µm. (B) Quantitation of immunostained cells on BM slides. Images of random HPFs were analyzed using an automated multispectral imaging microscope. Box and whisker plots of $CD45^+$, $CD68^+$, $CD90^+$, PM-$2K^+$, procollagen I^+, and dual-labeled cells (Merge) are depicted. The number of $CD90^+/CD45^-$ cells is the inverse of the merged data shown in the top right plot. The data shown are from BM and spleen samples from three patients (four slides/patient were analyzed). Boxes show the median and interquartile range, and whiskers denote the minimum and maximum data points. *, $P < 0.05$; **, $P < 0.01$ (Student's *t* test with Welch's correction comparing normal and PMF [merge]). (C) FISH images of a BM biopsy from the same patient showing $CD45^+/CD68^+$ cells (yellow) lacking one long arm of chromosome 20 ($20q^-$; cells showing only one red dot). Staining for chromosome 1 was used as an internal control (two green dots). Another field from the same BM specimen, depicting $20q^-$ cells, is shown at the bottom. Bars: (left) 50 µm; (right) 2.5 µm.

spleen sections from MPL-W515L mice that develop a PMF-like phenotype (Pikman et al., 2006). 2 wk after induction of MPL-W515L, large numbers of immature myeloid cells and dense megakaryocyte clusters with aberrant nuclear/cytoplasmic ratios and hyperchromatic and irregular nuclei were found in the BM and spleen (Fig. 6 A). In addition, a large number of cells coexpressing CD11b/procollagen I, CD45/procollagen I, and CD68/procollagen I were found in both the BM and spleen of MPL-W515L mice but not age-matched MPL-WT mice (Fig. 6, B–D). We then treated MPL-W515L mice with SAP (PRM-151) immediately after induction. Mice were initially given nine daily injections of 10 mg/kg SAP (PRM-151) and then twice weekly thereafter. Both placebo- and SAP (PRM-151)-treated

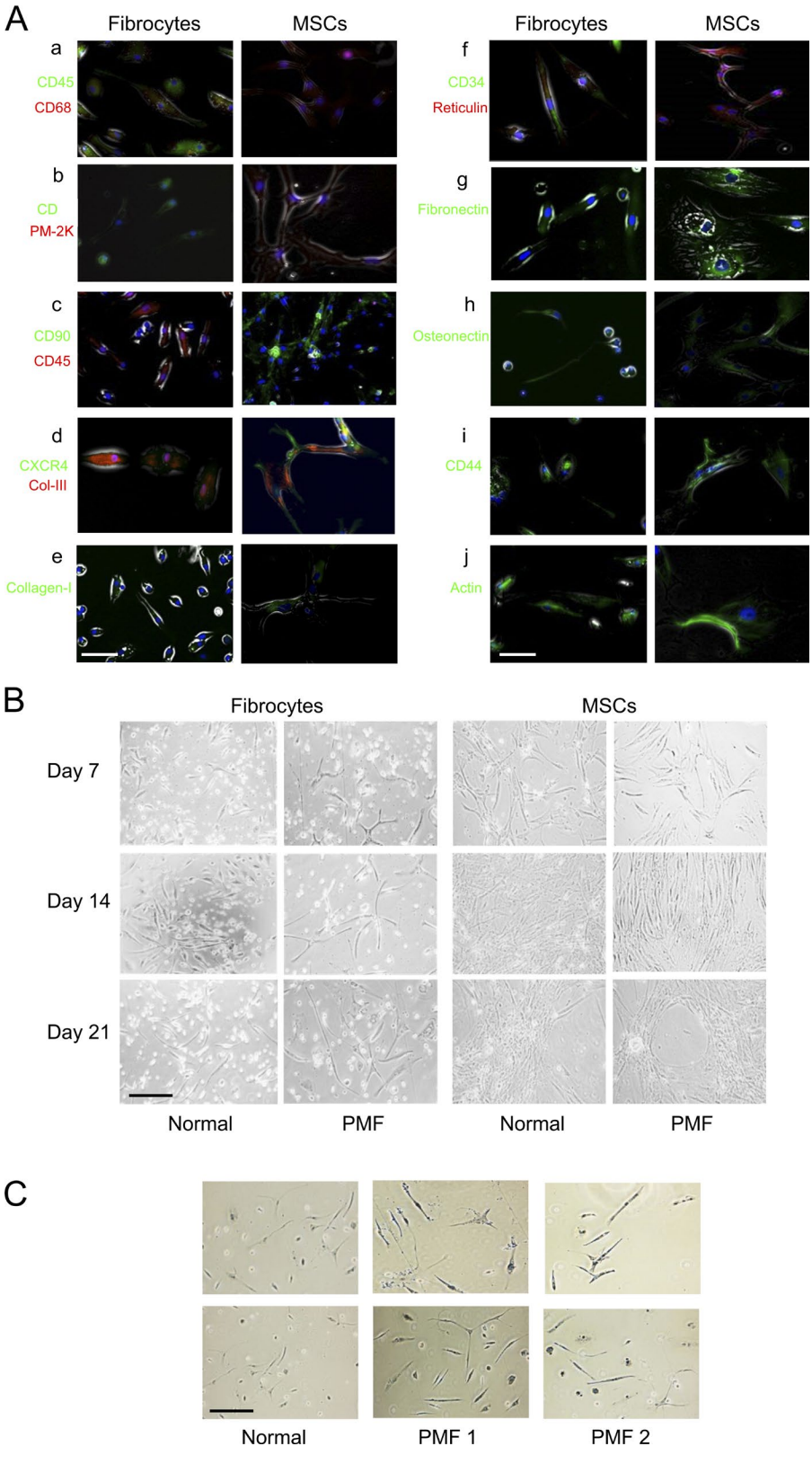

Figure 2. **Morphology of PMF and normal BM–derived fibrocytes.** (A) Immunofluorescence staining of PMF BM–derived fibrocytes and MSCs. (a) Costaining for CD45 and CD68. Fibrocytes were stained both by CD45 and CD68 antibodies (shown in light yellow), whereas MSCs were not stained by anti-CD45 antibodies. (b) Costaining for CD45 and PM-2K. Fibrocytes were stained by anti-CD45 but not by anti–PM-2K antibodies, whereas MSCs had no detectable staining for CD45 or PM-2K. (c) Staining for CD45 in fibrocytes and CD90 in MSCs. (d) Staining for both CXCR4 and collagen III (Col-III) is evident in both fibrocytes and MSCs. (e) Strong staining for collagen I in MSCs and weak staining in fibrocytes. (f) Staining for both CD34 and reticulin in fibrocytes but only reticulin in MSCs. (g) Staining for fibronectin in both fibrocytes and MSCs. (h–j) Staining for osteonectin, CD44, and actin in both fibrocytes and MSCs. Bars, 10 µm. DAPI staining is shown in blue. (B) Representative images of fibrocytes and MSCs grown from low-density BM cells of patients with PMF and hematologically normal donors. Images taken at day 7, 14, and 21 are depicted. Normal and PMF BM–derived fibrocytes are morphologically distinct from MSCs. Compared with normal BM–derived fibrocytes, PMF BM–derived fibrocytes are thicker, and their cytoplasmic extensions are more convoluted. Bar, 250 µm. (C) Silver staining in normal BM– and PMF-derived fibrocytes from two different patients showing that PMF BM–derived fibrocytes exhibit darker and thicker silver-stained cytoplasm, suggesting that they produce high levels of reticulin and/or type III collagen. Bar, 250 µm.

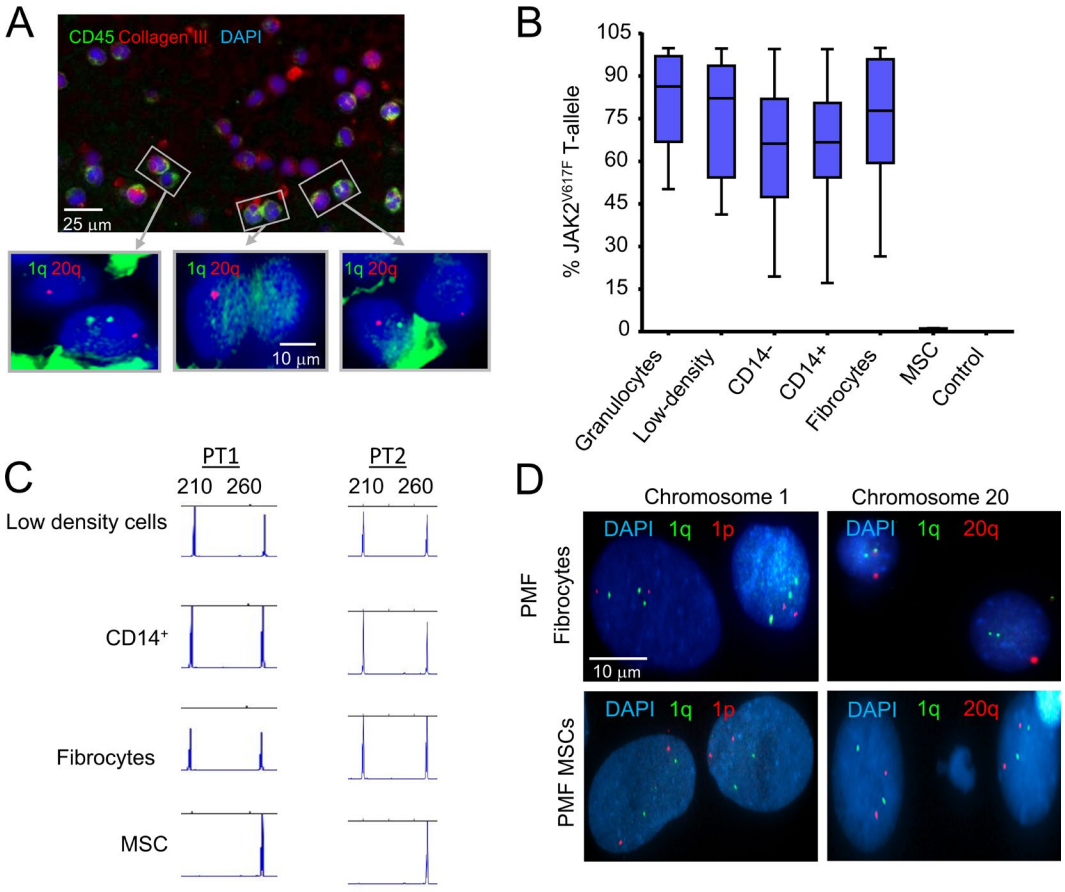

Figure 3. **PMF BM–derived fibrocytes originate from the neoplastic clone and are functionally distinct from normal fibrocytes.** (A) FISH images of a BM smear showing coexpression of CD45/collagen III in cells with the 20q deletion. (B) Median percentage of *JAK2* T allele in BM-derived cells from 12 PMF patients who tested positive for the *JAK2* mutation and seven BM and five PB samples from normal individuals (control). Boxes show the median, and interquartile range and whiskers denote the minimum and maximum data points. (C) Fragment analysis of the *CALR* gene showing the presence of a 52-bp deletion (peak at 210 bp) in BM mononuclear cells, $CD14^+$ cells, and fibrocytes but not MSCs from seven PMF patients known to harbor a *CALR* deletion. Representative data from two patients are shown. (D) Representative FISH images of MSCs and fibrocytes cultured from low-density BM cells from two patients with PMF who had either trisomy 1q (top left) or a 20q deletion (top right). FISH analysis was performed using 20q, 1q, and 1p probes.

mice died within 2 wk. However, BM and spleen specimens from SAP (PRM-151)-treated mice had much less fibrosis and significantly fewer fibrocytes than those from untreated mice (Fig. 6, E and F).

Engraftment of PMF BM cells in NOD-SCIDγ (NSG) mice

To determine whether BM fibrosis is induced by human fibrocytes, we generated a xenograft mouse model. In a series of similar experiments, we injected NSG mice with single-donor PMF or normal BM low-density cells. The PMF BM cells were obtained from seven patients with the JAK2-V617F mutation and cytogenetic abnormalities such as a 20q deletion, which could be interrogated by FISH. Engraftment of human BM–derived cells was confirmed by flow cytometry. All mice injected with human BM cells showed engraftment and had approximately the same percentage of $HLA\text{-}ABC^+$ cells throughout their life (Fig. 7 A and Table S4). Karyotype and FISH analyses performed after the mice became sick and were euthanized confirmed the presence of mouse and human chromosomes in mice injected with PMF BM (Fig. 7, B and C). The human chromosomes harbored the 20q deletion present in the BM PMF cells that were injected into mice. Rare (≤1%) cells with two copies of human chromosome 20 were also detected by FISH, suggesting that in addition to the PMF BM cells, donor-derived normal hematopoietic cells engrafted as well.

3 mo after injection of normal or PMF BM cells, two randomly selected mice from each cohort were euthanized. Mice injected with PMF BM low-density cells had enlarged spleens, whereas mice injected with normal BM had spleens that were similar in size to those of the IMDM-injected (control) mice (Fig. 7 D). BM sections from mice injected with PMF low-density cells were hypercellular with a high myeloid/erythroid (M:E) ratio and an increased number of

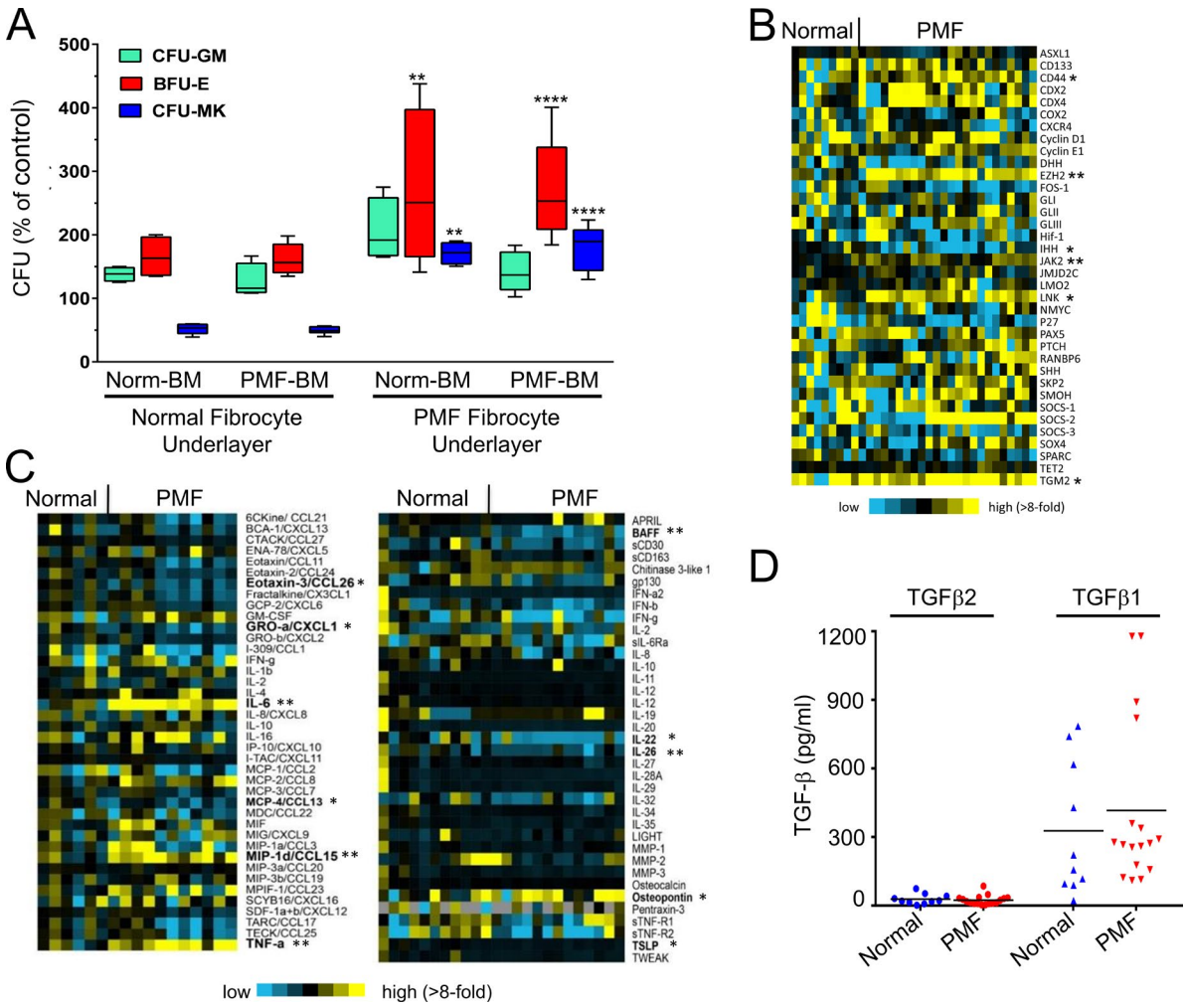

Figure 4. **Characterization of PMF and normal fibrocytes.** (A) The effect of normal- and PMF-derived adherent fibrocytes on hematopoietic colony-forming proliferation. Data shown are the number of burst units or CFUs as a percentage of the number of CFUs in the absence of a fibrocyte underlayer (control). The figure depicts data derived from experiments performed using fibrocyte underlayers derived from 12 normal and 22 PMF BM samples and an additional 6 normal (Norm) and 11 PMF BM samples to test colony formation. Each sample was tested in duplicate. The mean number of colonies in control normal BMs were: BFU-E, 2; CFU-GM, 83; and CFU megakaryocyte (CFU-MK), 9.2. Control PMF BM colonies were: BFU-E, 94; CFU-GM, 197; and CFU megakaryocyte, 30. Boxes show the median and interquartile range, and whiskers denote the minimum and maximum data points. Statistical differences were measured by one-way analysis of variance using Sidak's multiple comparisons test with an α of 0.05. **, $P < 0.01$; ****, $P < 0.0001$. (B) Heat map showing gene expression in PMF and normal fibrocytes. A colored gradient from blue (low expression) to yellow (high expression) is shown. Gene expression was measured in 24 PMF and 9 normal control samples. PMF fibrocytes have an increased expression of *JAK2*, *EZH2*, and *LNK*, which is likely associated with the $JAK2^{V617F}$ mutation. PMF fibrocytes also expressed higher levels of *CD44*, a cell surface glycoprotein involved in cell–cell interactions, cell adhesion, and cell migration (Maharjan et al., 2011), and lower levels of *IHH*, which has been shown to result in intestinal inflammation and fibrosis (van Dop et al., 2010). (C) Heat maps comparing levels of cytokines/chemokines secreted by PMF and normal fibrocytes. A colored gradient from blue (low levels) to yellow (high levels) is shown. 11 PMF and 6 normal samples were used. PMF fibrocytes secreted significantly higher levels of inflammatory cytokines (IL-6 and TNF) and chemokines (CCL15 and osteopontin) than normal fibrocytes. Differential expression was analyzed by Student's *t* test. *, $P < 0.05$; **, $P < 0.01$. (D) Levels of TGF-β1 and TGF-β2 secreted from cultured fibrocytes derived from BM from 17 PMF patients and 10 normal controls. Data are the mean of two measurements. Cytokine levels were measured by an enzyme-linked immunosorbent assay.

immature myeloid cells, blasts, and reticulin fibrosis. Their splenic architecture was markedly altered, and the spleens were infiltrated with left-shifted myeloid cells with increased blasts, a large number of immature atypical megakaryocytes, and marked reticulin fibrosis (Fig. 7 E, right). The BM of mice injected with normal BM cells were normocellular with a normal M:E ratio and morphologically normal megakaryocytes with no fibrosis. Their splenic architecture was preserved, with morphologically normal lymphocytes, a small number of myeloid cells, and a few megakaryocytes (Fig. 7 E, left).

Immunofluorescence analysis showed an overabundance of cells coexpressing CD68/CD45 and procollagen I/

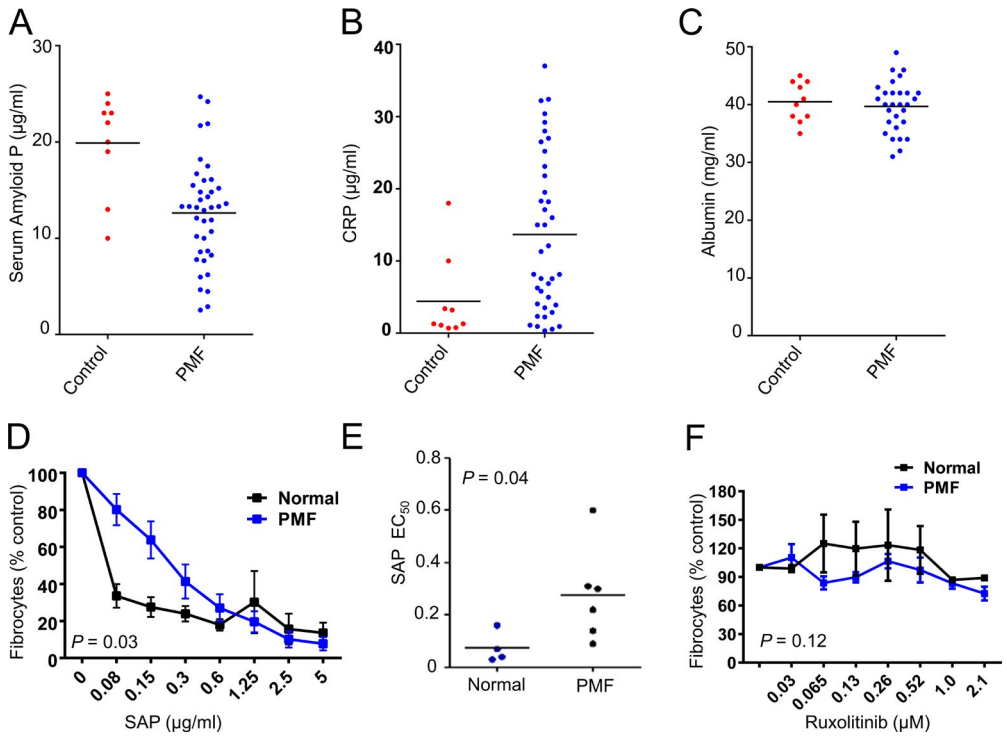

Figure 5. **Plasma levels of SAP, CRP, and albumin in PMF patients and effect of SAP and ruxolitinib on PMF and normal BM–derived fibrocytes.** (A–F) Levels of SAP (A), CRP (B), and albumin (C) in plasma samples from 39 patients with PMF and nine age-matched healthy individuals (control). (A) Data are mean ± SD. SAP levels in PMF (12.6 ± 5.39 µg/ml) and normal (21.4 ± 3.92 µg/ml) plasma samples ($P < 0.0006$) are shown. (B) Data are mean ± SD. CRP levels in PMF (13.38 ± 10.96 µg/ml) and normal (4.42 ± 1.96 µg/ml) plasma samples ($P = 0.019$) are shown. (C) Mean ± SD albumin levels in PMF (39.76 ± 4.55 mg/ml) and normal (40.5 ± 3.43 mg/ml) plasma samples ($P = 0.6$) are shown. Clinical characteristics of the 39 patients are shown in Table S1. (D and F) Increasing concentrations of SAP (PRM-151) (D) or ruxolitinib (F) were added to fibrocyte cultures 24 h after the initiation of cultures. After 7 d, the number of viable (morphologically intact and adherent to the bottom of the slide) fibrocytes/2.5 × 10^5 cells were counted independently by two individuals. Untreated cell cultures were used as a reference to calculate the percent viable fibrocytes. The mean ± SD of percent viable fibrocytes obtained from four (normal) or six (PMF) BM samples are depicted. Differences were calculated using two-way analysis of variance. The p-values reported are for variance by drug concentration. (E) A comparison of the EC_{50} of SAP between normal and PMF BM fibrocytes ($P = 0.038$; Mann-Whitney test). Unlike SAP in D, ruxolitinib did not affect fibrocyte differentiation in F. Four normal and six PMF BM samples were tested.

CD45 in the BM and to a lesser extent the spleens of mice injected with PMF BM cells (Fig. 8 A) but not those injected with normal BM cells (Fig. 8 B). Although macrophages also coexpress CD45/CD68, they could be distinguished from fibrocytes by their size and morphology. In addition, the number of $CD68^+/CD45^+$ and procollagen $I^+/CD45^+$ cells per square millimeter in engrafted BM (Fig. 8 C, top) and spleens (Fig. 8 C, bottom) was significantly higher in mice injected with PMF cells than in those injected with normal BM cells. 11% of the BM low-density cells harvested from mice injected with PMF BM cells coexpressed $CD68^+/CD45^+$ as assessed by flow cytometry (Fig. 8 D), and fibrocytes cultured from these cells carried the 20q-cytogenetic abnormality present in the injected BM cells from the patient, implying that these fibrocytes originated from the human neoplastic clone (Fig. 8 E).

SAP (PRM-151) extends survival of xenograft mice

Because SAP (PRM-151) inhibited PMF fibrocyte differentiation in culture (Fig. 5 D), we investigated whether it would inhibit the development of BM fibrosis in our xenograft mouse model. As a pilot experiment, 20 NSG mice transplanted with BM low-density cells from a PMF patient were injected intraperitoneally with 10 mg/kg SAP (PRM-151) or the drug's vehicle (placebo) starting the day after BM transplantation according to the treatment schedule shown in Fig. 9 A. By day 241, all 10 placebo-treated NSG mice had died, whereas all 10 mice in the SAP (PRM-151)–treated group were still alive and healthy (Fig. 9 B).

To determine whether SAP could slow or reverse BM fibrosis, an additional 30 NSG mice were transplanted with low-density cells from another PMF patient harboring the $JAK2^{V617F}$ mutation and a 20q deletion. The mice were randomized into three treatment groups as follows: (group A) 10 mice were injected intraperitoneally with 10 mg/kg SAP (PRM-151) as described in the previous paragraph starting 2 wk after transplantation; (group B) 10 mice received SAP (PRM-151) starting 2 mo after transplantation; and (group C, placebo) 10 mice were injected intraperitoneally with the

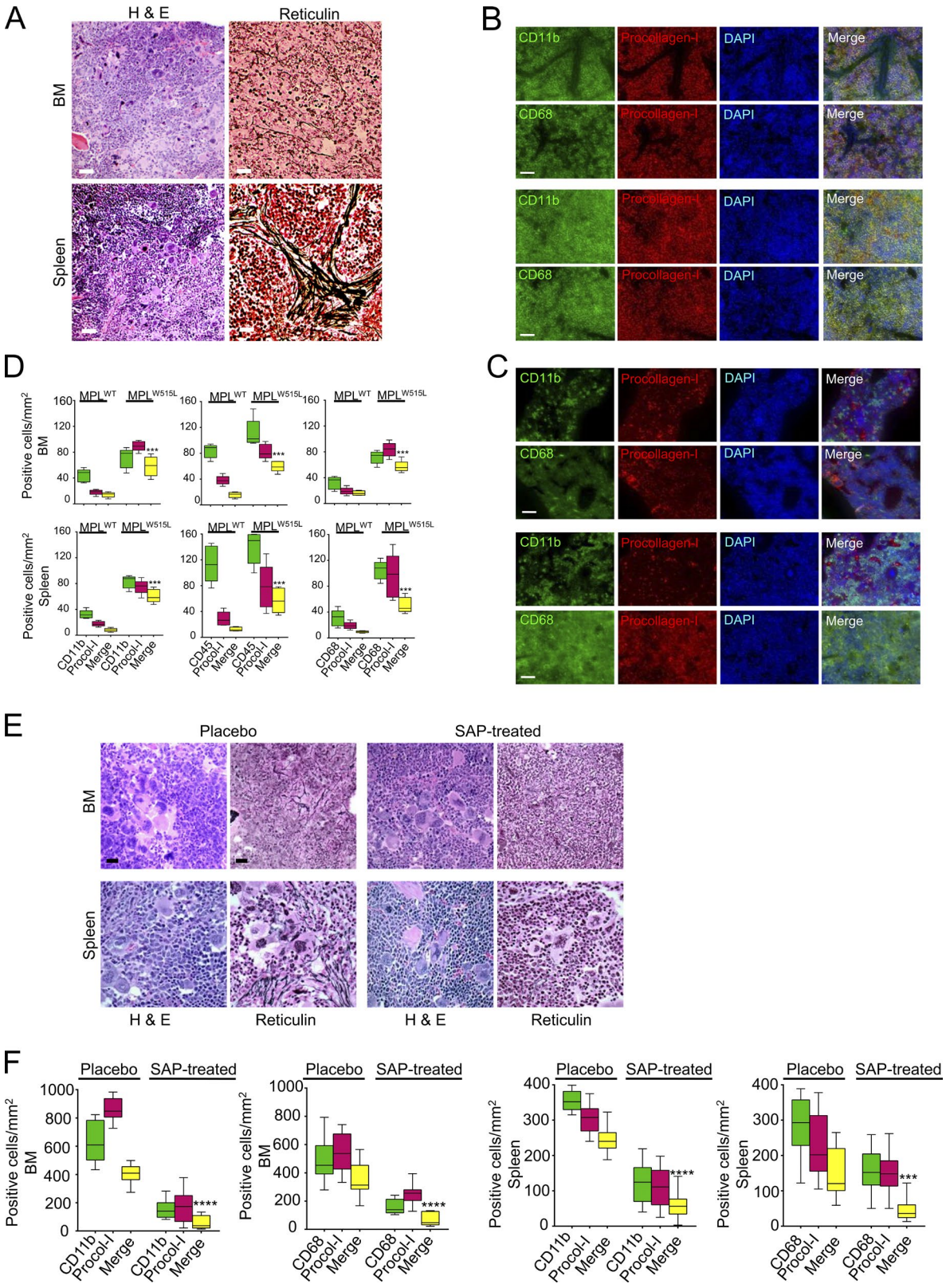

Figure 6. **BM analysis of untreated and SAP (PRM-151)–treated MPL-W515L mice.** (A) H&E and reticulin staining images of femur and spleen sections from MPL-W515L–induced myelofibrosis mice. Images are representative of tissue sections from seven mice. The mean fibrosis grade was MF-3. Large numbers of immature myeloid cells and dense clusters of small to large megakaryocytes with aberrant nuclear cytoplasmic ratios and hyperchromatic

placebo (the vehicle of PRM-151) starting 2 wk after transplantation (Fig. 9 A). At the same time, 10 nontransplanted, untreated NSG mice were monitored (control). All transplanted, placebo-treated NSG mice lost weight (Fig. 9 C), became sick and moribund, and were euthanized, whereas all SAP (PRM-151)–treated or control (nontransplanted or normal BM transplanted) mice were alive and healthy during this period (Fig. 9 D).

All transplanted, placebo-treated mice had leukocytosis, anemia, and thrombocytosis (Fig. 9 E), and on necropsy, they had marked splenomegaly, and their BM and spleens were heavily infiltrated with immature myeloid cells and atypical megakaryocytes. Extramedullary hematopoiesis was occasionally detected in their lungs (not depicted), whereas their livers appeared morphologically intact, and none of the mice had blastic transformation. However, dilated sinusoids, intrasinusoidal hematopoiesis, and BM and spleen fibrosis were detected in all sections (Fig. 10, B and C). A granuloma was seen in one splenic section (Fig. 10 C).

On day 239 after transplantation when all placebo-treated mice had become sick and been euthanized, two SAP-treated mice from group A, two from group B, and two nontransplanted mice (control) were euthanized. None of these mice showed external signs of illness at the time of sacrifice. Their spleen sizes were similar to those of the nontransplanted age-matched mice (Fig. 10 D). Mouse–human chimerism was detected by FISH in all SAP (PRM-151)– and placebo-treated mice but not the nontransplanted controls (Fig. 10 A). Unlike placebo-treated mice, in mice that started treatment at 2 wk (group A), only mild focal BM and spleen fibrosis was detected. The BM megakaryocytes appeared normal, and although myeloid cells were detected in their spleens, the splenic architecture was largely preserved (Fig. 10 B, second panel from the right). Similarly, in mice that started treatment at 2 mo, BM and spleen sections showed clusters of hyperchromatic megakaryocytes and diffuse areas of mild reticulin fibrosis (Fig. 10 B, group B). In contrast, tissue sections from the nontransplanted untreated mice showed a normal splenic architecture and normal spleen and BM morphology (Fig. 10 B, control). As expected, the number of fibrocytes in BM and spleen ($CD45^+/CD68^+$ and $CD45^+$/procollagen I^+ cells) tissues from the SAP (PRM-151)-treated mice was significantly lower than the number in those of placebo-treated mice (Fig. 10 E). In addition, SAP (PRM-151)–treated mice had normal white blood cell (WBC) counts and hemoglobin levels, though their platelet counts remained high (Fig. 9 E). There were no obvious changes in BM cellularity or megakaryocyte counts after SAP (PRM-151) treatment. 8 mo after injection of BM cells, we discontinued treatment with SAP, and all mice died of PMF without transformation to acute leukemia (Fig. 10 F), indicating that continued treatment with SAP (PRM-151) was necessary to inhibit the development of the myelofibrosis-like phenotype in xenograft mice.

DISCUSSION

BM fibrosis in PMF is presumed to be caused by growth factors released from clonal megakaryocytes or platelets that stimulate MSCs to induce BM fibrosis (Groopman, 1980). Here, we demonstrate that clonal neoplastic fibrocytes, which are significantly expanded in patients with PMF, are functionally distinct from normal fibrocytes (perhaps because of constitutive JAK2 signaling) and contribute to the formation of BM fibrosis. Furthermore, SAP (PRM-151) slowed the development of fibrosis and significantly improved survival of NSG mice transplanted with PMF BM cells.

That fibrocytes play a direct role in the induction of BM fibrosis is not unprecedented. Ohishi et al. (2012) found an expanded population of $CD45^+$ cells that produced type I collagen (fibrocytes) in the BM of mice conditionally expressing active parathyroid hormone receptor, results that are reminiscent of our data obtained from the mouse MPL-W515L–induced PMF model. In the parathyroid hormone receptor mice, the numbers of MSCs in BM from control mice and mice with hyperparathyroidism-induced BM fibrosis were similar. Similar to our findings, Arranz et al., 2014 found a reduced number of MSCs in BM specimens of JAK2-V617F–positive myeloproliferative neoplasm patients and mice expressing JAK2-V617F in the hematopoietic system (Tiedt et al., 2008). Consistent with our data, the reduction in MSCs was concomitant with the formation of BM fibrosis in mice, suggesting that other cells rather than MSCs are the major contributors to the formation of BM fibrosis in myeloproliferative neoplasms.

and irregular nuclei in both the BM and spleen are shown. In both tissues, significant reticulin fibrosis was detected by reticulin staining. Bars: (H&E) 100 µm; (reticulin) 50 µm. (B and C) BM (top) and spleen (bottom) sections from MPL-W515L–induced MF mice (B) and control mice (MPL-WT; C) stained for CD11 and procollagen I and CD68 and procollagen I. Unlike the WT (control) mice, BM and spleen cells from MPL-W515L mice stained positively for CD11/procollagen I (yellow; top, bottom right) and CD68/procollagen I (yellow; bottom, bottom right). Results are representative of two MPL-W515L mice and two MPL-WT mice. Bars, 50 µm. (D) Quantitation of immunostained cells in BM and spleen sections. Images of random HPFs of four slides from four different mice were analyzed using an automated multispectral imaging microscope. Box and whisker plots of $CD11b^+$, $CD45^+$, $CD68^+$, procollagen I^+ (Procol-I), and dual-labeled cells (merge) per square millimeter are shown. Boxes show the median and interquartile range, and whiskers denote the minimum and maximum data points. ***, $P < 0.001$ (Student's *t* test comparing MPL-WT and MPL-W515L [merge]). (E) BM and spleen sections from MPL-W515L mice treated with either placebo or SAP. Images are representative of tissue sections from seven placebo-treated mice and six SAP-treated mice. The mean fibrosis grade was MF-3 in placebo-treated mice, and SAP-treated mice ranged from MF-0 to MF-1. Both placebo- and SAP-treated sections showed hypercellularity, a high M:E ratio, and atypical megakaryocytes and blasts. However, placebo-treated mice had much more BM fibrosis than the SAP-treated mice, which hardly had any. Bars: (H&E) 100 µm; (reticulin) 50 µm. (F) Quantitation of immunostained cells in BM and spleen sections of placebo- and SAP (PRM-151)–treated MPL-W515L mice. Data are presented as in D. ****, $P < 0.0001$.

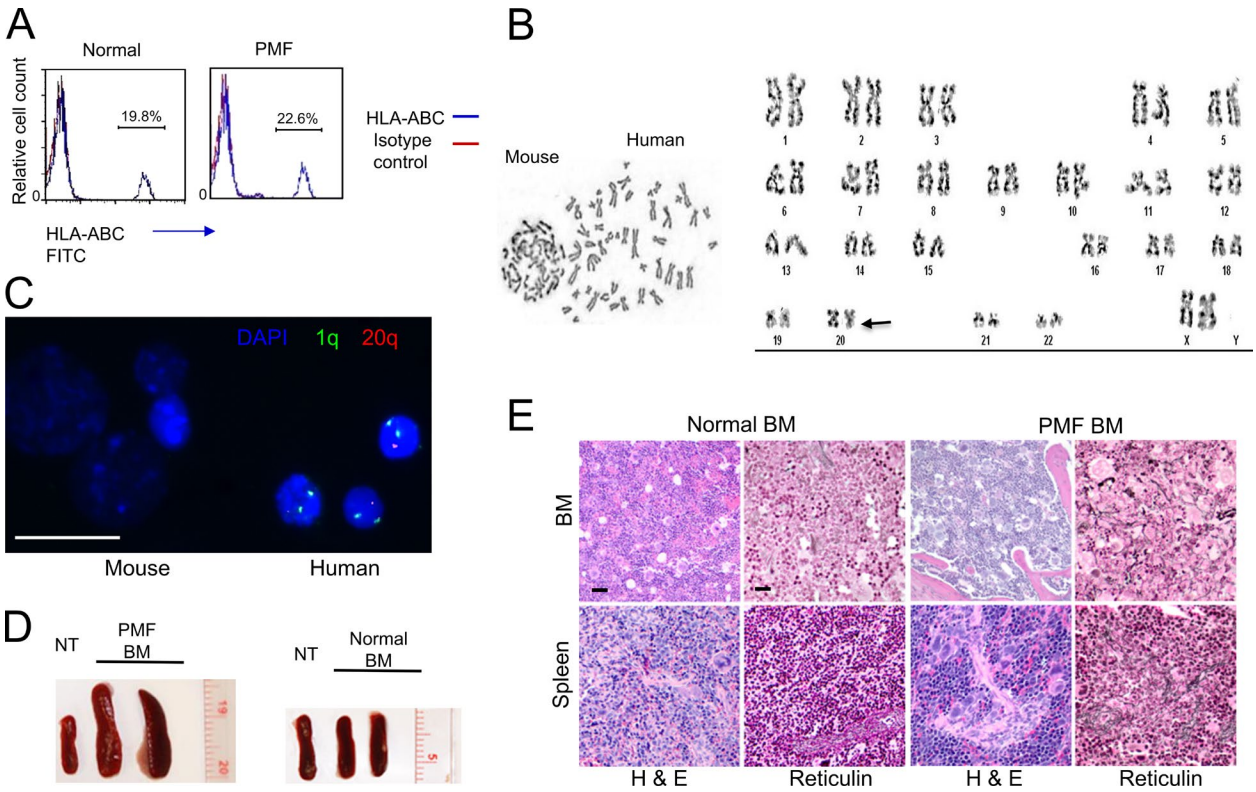

Figure 7. **Engraftment of human PMF BM–derived cells in NSG mice.** (A) Representative flow cytometry plot of PB from NSG mice injected with normal human or PMF BM–derived low-density cells showing the presence of cells carrying the HLA-ABC antigen. PB cells were assessed 14 d after injection of BM cells and approximately every 2–4 wk thereafter to confirm the mouse–human chimerism. Approximately the same level of HLA-ABC–positive cells was detected throughout the animal's life (Table S4). (B) Karyotype (Giemsa banding) analysis of BM cells obtained from NSG mice injected with PMF BM–derived low-density cells. The arrow indicates the 20q deletion in the human cells. (C) FISH analysis of BM cells from xenograft mice using probes specific for 20q and 1q (internal control). DAPI nuclear staining is shown in blue. Both mouse and human cells are depicted. Bar, 10 µm. (D) Mouse spleens 3 mo after injection of PMF or normal BM low-density cells. Spleens from nontransplanted (NT) mice are shown for comparison. (E) H&E and reticulin staining of BM (femur) and spleen sections of mice injected with normal or PMF BM low-density cells. Notable features in PMF include atypical megakaryopoiesis anisocytosis, abnormal large nuclear/cytoplasmic ratio, hyperchromatic nuclei, and plump lobulation of the nuclei. Reticulin-stained BM sections from mice injected with PMF BM cells shows increased reticulin fibrosis. In contrast, in mice injected with normal BM cells, hematopoiesis is unaltered, splenic architecture is preserved, and no significant reticulin fiber deposition is observed. Images are representative of 10 mice injected with normal BM cells and 10 injected with PMF BM cells. The fibrosis grade ranged from MF-2 to MF-3 in PMF BM–injected mice, and no fibrosis was seen in any of the normal BM–injected mice. Bars: (H&E) 100 µm; (reticulin) 50 µm.

To test our hypothesis that fibrocytes mediate the induction of fibrosis in PMF, we transplanted NSG mice with PMF BM–derived low-density cells. Because low-density BM cells from patients with chronic myelogenous leukemia have been shown to engraft NSG mice (Verstegen et al., 1999), PMF-derived $CD34^+$ cells have been shown to induce acute myeloid leukemia but not PMF in NSG mice (Triviai et al., 2014), and $CD34^-$ cells have been shown to engraft NSG mice (Bhatia et al., 1998; Zanjani et al., 1998), we opted to inject mice with unfractionated low-density cells to avoid excluding any cellular population that may be important for engraftment or the establishment of human PMF in mice. As in human PMF BM and the BM and spleen of MPL-W515L mice, the fibrotic hematopoietic tissue of the xenograft mice was characterized by a massive expansion of clonal fibrocytes. Although low-density cells from normal BM also engrafted, few BM fibrocytes were detected, and the mice did not develop PMF.

In both PMF mouse models, we found increased numbers of atypical megakaryocytes, a defining pathological feature of PMF. Interestingly, TGF-β, which is highly expressed in megakaryocytes from patients with PMF (Martyré et al., 1997), has been shown to play a role in fibrocyte differentiation (Hong et al., 2007). Thus, megakaryocyte-derived cytokines may in fact promote fibrosis, but more likely by promoting differentiation of fibrocytes.

SAP has been shown to inhibit the differentiation of fibrocytes from monocytes and to reduce fibrosis in various organs (Haudek et al., 2006, 2008; Pilling et al., 2007; Castaño et al., 2009; Murray et al., 2011; Reilkoff et al., 2011). In addition, SAP promotes immunoregulatory macrophages that secrete IL-10, which is known to modulate fibrosis (Castaño

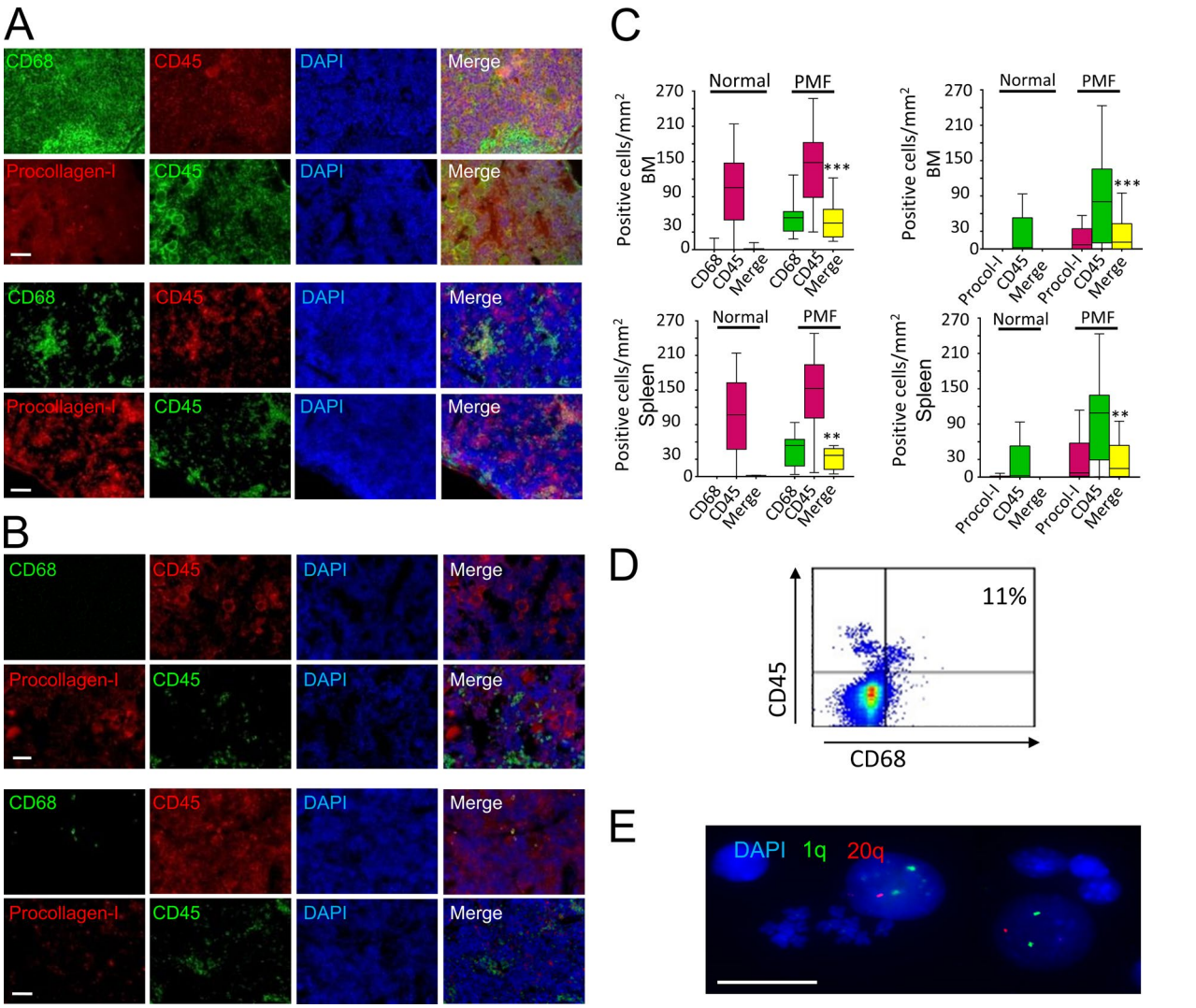

Figure 8. **Quantitation of clonal fibrocytes in xenograft mice.** (A and B) Immunohistochemical staining of BM (top) and spleen (bottom) sections of mice injected with PMF BM–derived low-density cells (A) or normal human BM–derived low-density cells (B). Bars, 50 µm. (C) Quantitation of immunostained cells in BM and spleen sections. Images of five random HPFs per slide were analyzed using an automated multispectral imaging microscope. Data represent analysis of five slides from five different animals. Box and whisker plots of $CD45^+$, $CD68^+$, procollagen I^+ (Procol-I), and dual-labeled cells (Merge) per square millimeter are shown. Boxes represent the median and interquartile range, and whiskers denote the minimum and maximum data points. **, $P < 0.01$; ***, $P < 0.001$ (Student's *t* test with Welch's correction comparing normal and PMF [merge]). (D and E) Clonality assessment of fibrocytes from mice injected with PMF-derived BM cells. (D) Representative flow cytometry dot plot showing that 11% of cells flushed from the femurs of xenograft mice injected with BM low-density cells from a PMF patient with a 20q deletion coexpressed human $CD45^+/CD68^+$ antigens. (E) FISH image of fibrocytes cultured from BM cells harvested from the same xenograft mice shows the presence of the 20q deletion in the cultured fibrocytes. Bar, 10 µm.

et al., 2009; Cox et al., 2015). We found that patients with PMF had low plasma SAP and high plasma CRP levels compared with healthy individuals, suggesting that the low SAP levels in PMF patients are less likely to be caused by reduced production than by increased consumption and clearance (Bottazzi et al., 2010).

Our finding that SAP (PRM-151) significantly prolonged the life of PMF xenograft mice and slowed the formation of BM fibrosis provides compelling evidence that hematopoietic tissue fibrosis is induced by fibrocytes and suggests that SAP may inhibit or reverse BM fibrosis in patients with myelofibrosis. Indeed, the number of fibrocytes was markedly reduced in the BM and spleens of SAP-treated compared with placebo-treated mice. Furthermore, the total number of WBCs and $CD45^+$ cells was also reduced in SAP-treated mice, suggesting that neoplastic fibrocytes may directly or indirectly sustain the neoplastic clone or that SAP has another yet undefined mechanism of action (Kleaveland et al., 2014). Discontinuation of treatment, however, led to reestablishment of PMF and eventual death of the transplanted mice.

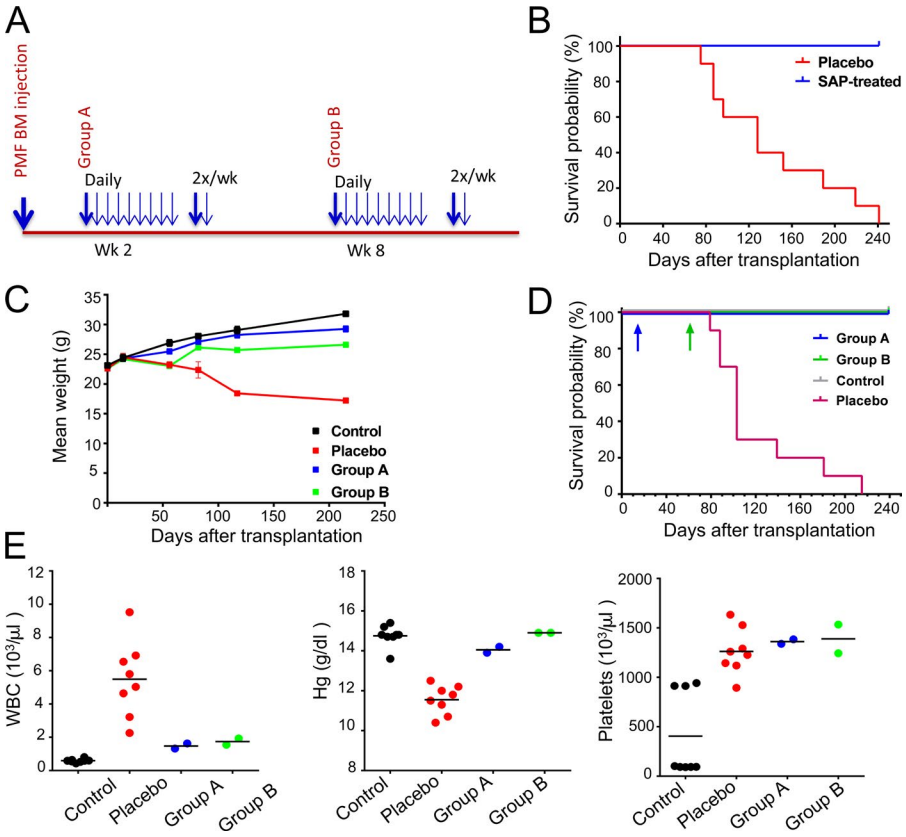

Figure 9. **Characterization of xenograft mice treated with SAP.** (A) SAP (PRM-151) treatment schedule. Mice were injected with 10 mg/kg daily for the first 9 d and then twice per week thereafter. (B) Kaplan-Meier survival analysis of 10 mice treated with placebo and 10 treated with SAP starting the day after injection of PMF BM cells. (C) Plot showing mean ± SEM change in the weight of nontransplanted (control), placebo-treated (placebo), and SAP-treated (group A and group B) PMF BM–transplanted mice. Weight was measured at six different time points. (D) Kaplan-Meier survival analysis of xenograft mice treated with placebo or SAP 2 wk (group A) or 2 mo (group B) after injection of PMF BM cells. Arrows indicate times of treatment initiation. Placebo-treated mice were euthanized in accordance with our institutional protocol 79 (n = 1), 88 (n = 2), 103 (n = 5), 181 (n = 1), and 205 (n = 1) d after transplantation. With 10 mice per group and assuming a 10% survival rate for the placebo group and 90% for the treatment groups, we have 82% power with a type 1 error rate of 0.05% to test our hypothesis that mice treated with SAP live significantly longer than those treated with the placebo. (E) PB counts of control (n = 10), placebo-treated (n = 8), and SAP-treated (n = 4, 2 in group A and 2 in group B) mice obtained before the placebo-treated mice were euthanized. Black lines represent the median. Unlike placebo-treated mice, SAP (PRM-151)–treated mice did not have anemia, and the WBC counts were normalized. However, the platelet counts of SAP-treated mice remained high, similar to the placebo-treated mice.

MATERIALS AND METHODS

Samples and cell fractionation

We used diagnostic BM samples that were obtained before treatment from patients with PMF treated at the University of Texas MD Anderson Cancer Center during a 4-yr period. Institutional Review Board approval and written patient informed consent were obtained. The clinical characteristics of the patients are presented in Table S1. Hematologically normal BM and peripheral blood (PB) samples were purchased from STEMCELL Technologies for comparison. BM and PB cells were fractionated using Ficoll Hypaque 1077 (Sigma-Aldrich). After the buoyant low-density cells were aspirated, a red blood cell lysis buffer (QIAGEN) was added for 5 min, and the remaining granulocytes were harvested and washed in PBS (Invitrogen). $CD14^+$ and $CD14^-$ cells were selected from the low-density cell fraction using EasySep magnetic microbeads (STEMCELL Technologies) according to the manufacturer's instructions.

Fibrocyte cell culture assay

Low-density BM cells were cultured in conditions that promote differentiation of monocytes to fibrocytes (Pilling et al., 2003) as described previously (Pilling et al., 2009). In brief, $CD14^+$ monocytes purified from low-density BM cells (purity >97%) were cultured with serum-free medium (StemPro-34; Invitrogen) supplemented with 10 mM 4-(2-hydroxyethyl)-1-piperazineethanesulfonic acid (Sigma-Aldrich), 1× nonessential amino acids (Sigma-Aldrich), 1 mM sodium pyruvate (Sigma-Aldrich), 2 mM glutamine (Invitrogen), 100 U/ml penicillin, 100 µg/ml streptomycin, and 1× ITS-3 (containing 10 µg/ml insulin, 5 µg/ml transferrin, 5 ng/ml sodium selenite, 0.5 mg/ml albumin, 5 µg/ml oleic acid, and 5 µg/ml linoleic acid [Sigma-Aldrich]), either in flat-bottomed 96-well plates or in Lab-Tek microscope chamber slides (CC2 slides; Thermo Fisher Scientific). Culture plates and slides were maintained at 37°C in humidified air supplemented with 5% CO_2.

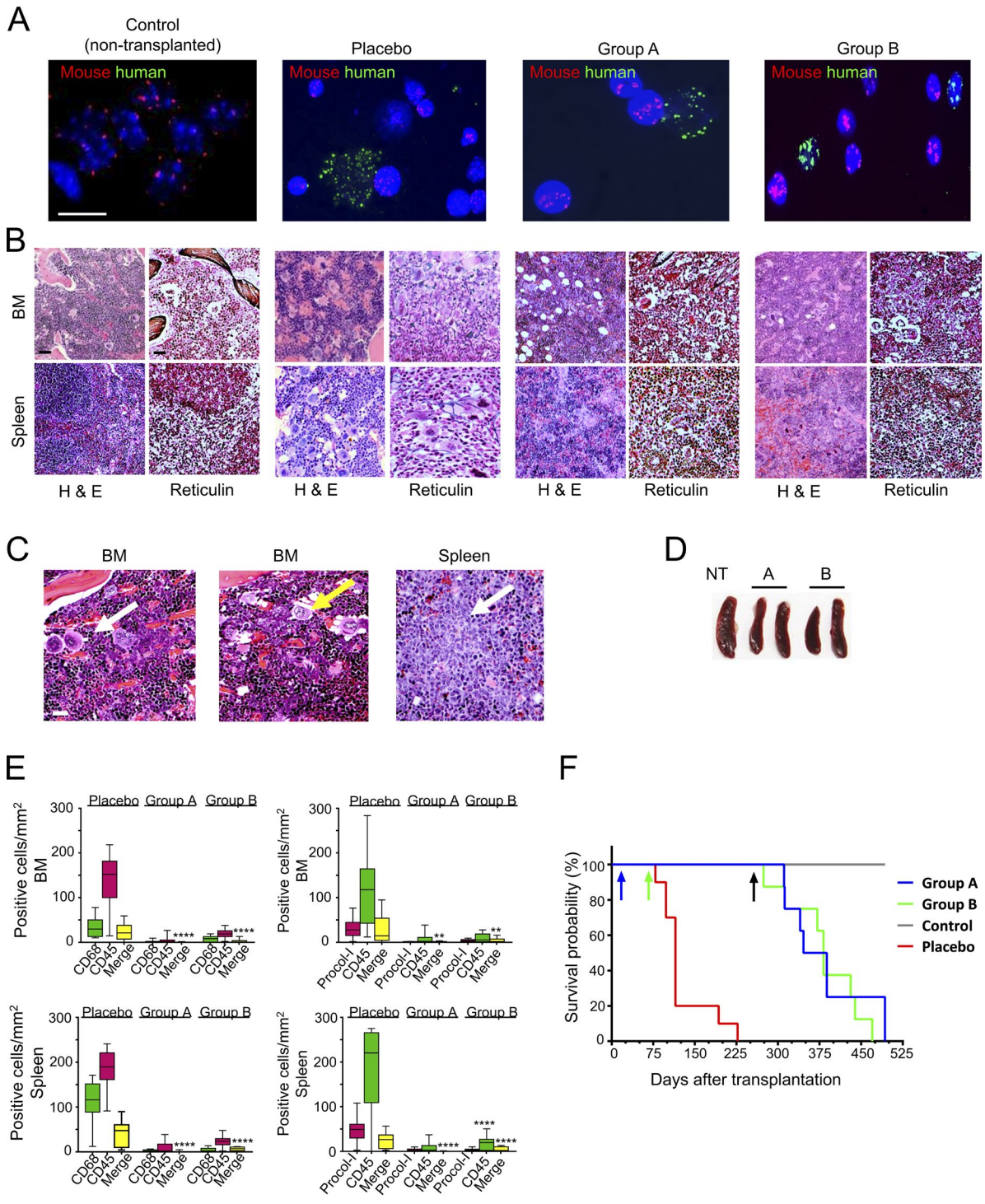

Figure 10. **Characterization of xenograft mice treated with SAP either before or after the development of BM fibrosis.** (A) FISH analysis of BM sections from normal, nontransplanted, untreated mice (left) or PMF BM–transplanted mice treated with SAP 2 wk after transplantation (group A) or 2 mo after transplantation (group B) using probes for human and mouse centromeres. Cells harboring human centromeres were detected in 10% of the analyzed slides. Bar, 10 µm. (B) Representative H&E and reticulin staining of femur and spleen sections from a nontransplanted normal, age-matched control mouse, a PMF BM–transplanted placebo-treated mouse, and a PMF BM–transplanted mouse treated with SAP (PRM-151) starting either 2 wk (group A) or 2 mo (group B) after transplantation. Bars: (H&E) 100 µm; (reticulin) 50 µm. (C) H&E staining of BM and spleen sections from transplanted, placebo-treated NSG mice showing numerous atypical megakaryocytes, some of which were present within the sinuses (left, white arrow), dilated sinusoids, intrasinusoidal hematopoiesis with evolving myelofibrosis (yellow arrow), and an increase in immature myeloid cells. (Right) The spleen section shows myeloid sarcoma

Cells were visualized using a phase-contrast microscope (ELWD 0.3; 10/0.25 objective lens; Nikon), photographed using a digital camera (D40; Nikon), and counted as previously described (Pilling et al., 2003; 2009). The number of fibrocytes generated in culture varied by patient sample but ranged from 200 to 400 cells.

MSC culture assay

BM cells from patients with PMF and healthy donors were cultured in conditions that support MSC proliferation. Low-density BM cells (10^6 cells/ml) were cultured in α-modified Eagle's medium (Invitrogen) supplemented with 20% FCS (Invitrogen). The medium was replenished twice weekly. For further analysis, adherent MSCs were washed with PBS, pH 7.4, and removed after incubation with 0.25% trypsin (Sigma-Aldrich) for 5–7 min. Cultures were photographed and manually assessed at days 7, 14, and 21 as described for the cultured fibrocytes in the previous section.

Immunofluorescence

Paraffin-embedded 4-µm BM biopsy sections were oven dried for 1 h at 56°C, deparaffinized, rinsed three times in xylene, and rehydrated using graded concentrations of ethanol (100%, 90%, 80%, and 70%), and the epitopes were retrieved with Diva decloaker buffer in a decloaking chamber using the Mach-3 system (Biocare Medical). Cells were cultured in 8-well microscope chamber slides for 14 d, washed with PBS, and fixed in 4% formaldehyde. Slides were washed in PBS and incubated with primary antibodies at a predetermined concentration (Table S2) for 3 h at room temperature, and BM sections were incubated for 12 h with primary antibodies in blocking buffer in a humidified chamber on a shaker at 4°C. Slides were then washed in PBS and incubated with Alexa Fluor–conjugated antibodies (Table S2; Invitrogen) for 1 h at room temperature, washed in PBS, and counterstained with DAPI (Invitrogen). Antifade fluorescent mounting medium (Dako) was added, and the coverslip was applied.

Images were captured using a 20×/0.9 objective lens mounted on a microscope (Exfo; ZEISS) and recorded and processed using AxioVision software (ZEISS). For quantitative analysis, images were analyzed using a Vectra 2 (I × 81; Olympus) automated multispectral imaging microscope (PerkinElmer). High-power fields (HPFs; 40×) were manually chosen, with at least 25 fields per sample. Data were analyzed using inForm software (PerkinElmer). Normalization and background correction were performed using an unstained slide and a slide stained with the secondary antibody/DAPI to generate an analysis library. Randomly selected HPFs from four different slides were analyzed for each BM sample. Samples from three patients and three controls were analyzed in each experiment.

Silver staining for reticulin fibers

The reticulin silver Chromaview advance testing kit (Richard-Allen Scientific) was used for staining BM-derived cultured fibrocytes and MSCs in accordance with the manufacturer's instructions.

DNA extraction and quantitation of the *JAK2* mutant T allele and CALR mutation

Granulocytes, low-density BM cells, cultured BM-derived fibrocytes, and MSCs from patients with PMF known to harbor either the *JAK2* (n = 12) or *CALR* (n = 7) mutations were tested for the presence of these mutations. We also examined the mutation status of seven normal BM samples and five normal PB samples as a control. Fibrocytes and MSCs were cultured as described in the Fibrocyte cell culture assay and MSC culture assay sections. After 14 d in culture, the adherent fibrocytes or MSCs were washed three times with PBS, pH 7.4, to remove the nonadherent cells. Puregene DNA lysis buffer was then added directly to the adherent cells. Genomic DNA was extracted using Puregene DNA purification reagents (Gentra). Total genomic DNA was used for PCR amplification of *JAK2* exon 14, and quantitative allele-specific suppressive PCR was performed as described previously (Quintás-Cardama et al., 2011). Insertions or deletions in the *CALR* gene were analyzed by PCR fragment analysis as previously described (Klampfl et al., 2013).

FISH

Slides of BM fibrocytes, MSCs, and mouse and human BM tissue were washed in PBS and dehydrated in ethanol, as described for the BM biopsy specimens in the Immunofluorescence section, and treated with RNase for 1 h at 37°C. Slides

with numerous blasts disrupting the splenic architecture (white arrow). Images are representative of tissue sections from 10 nontransplanted mice, 10 PMF BM–transplanted placebo-treated mice, and two SAP-treated mice from group A and two from group B. The BM fibrosis grade ranged as follows: nontransplanted, no fibrosis; placebo, MF-2 to MF-3; group A, no fibrosis; and group B, MF-0 to MF-1. Bar, 100 µm. (D) Spleens of SAP-treated mice from group A (A) and group B (B) and an age-matched nontransplanted (NT) mouse. Spleen weights were as follows: nontransplanted group, 0.09–0.105 g; placebo group, 0.165–0.224 g with one spleen weighing 31.8 g; group A, 0.083–0.101 g; and group B, 0.092–0.112 g. (E) Quantitation of immunostained cells in BM and spleen sections. Images are of random HPFs of four different slides from four animals for the placebo group, two animals for group A, and two animals for group B analyzed using an automated multispectral imaging microscope. Box and whisker plots of $CD45^+$, $CD68^+$, procollagen I^+ (Procol-I), and dual-labeled cells (Merge) per square millimeter are shown. Boxes represent the median and interquartile range, and whiskers denote the minimum and maximum data points. **, $P < 0.01$; ****, $P < 0.0001$ (Student's t test with Welch's correction comparing placebo vs. group A or group B [merge]). (F) Kaplan-Meier survival analysis of mice treated with placebo (n = 10) or SAP 2 wk (n = 10; group A, blue arrow) or 2 mo (n = 10; group B, green arrow) after injection of PMF BM cells showing survival after the discontinuation of SAP treatment (day 247; black arrow). 10 nontransplanted, untreated mice were used as a control group. All mice in both groups became sick and were sacrificed 311–470 d after injection of PMF BM cells.

were then incubated with 2× saline-sodium citrate (SSC) buffer (0.3 M sodium chloride and 30 mM sodium citrate, pH 7.0) for 30 min, left overnight in 1 M sodium isothiocyanate, and rinsed with 2× SSC. Slides were treated with 4 mg/ml pepsin (Vysis; Abbott Molecular) at 37°C, washed in 2× SSC at room temperature, dehydrated with 70% ethanol, and air dried. A mixture of probes (Abbott Molecular) detecting chromosomes 1p, 1q, or 20q, human centromeres, or mouse centromeres was denatured at 74°C for 5 min and applied to the cells. Slides were sealed with a coverslip and rubber cement (Thermo Fisher Scientific) and incubated overnight at 37°C in a humidified atmosphere. The coverslips were then removed, and the slides were washed in 2× SSC at 45°C for 30 min, counterstained with 1 μg/ml DAPI, and mounted with antifade mounting medium (Dako). Fluorescence-specific signals were visualized by fluorescence microscopy, and the images were captured at a magnification of 100 with a microscope (Eclipse 80i; Nikon) equipped with a Photometrics SenSys charged-coupled device camera (Roper Technologies). Images were analyzed using Metamorph software (Molecular Devices). The analysis was performed with coded BM samples in a core pathology laboratory at our institution, and the pathologist had no knowledge of the origin of the slides. A cell was considered positive for the chromosomal marker only in cases where the internal control probe was also visualized.

Clonogenic assays

Normal and PMF BM low-density cells were incubated in methylcellulose alone as previously described (Estrov et al., 1987) or on top of a preestablished adherent layer of a similar number of normal and PMF BM–derived fibrocytes. For the adherent under layer, fibrocytes were cultured from normal or PMF BM low-density cells as described previously (Pilling et al., 2003, 2009). The adherent fibrocytes were washed three times with PBS, pH 7.4, to remove the nonadherent cells, and then the BM low-density cells were placed on top of them. In brief, 2×10^5 low-density cells were mixed in 0.8% methylcellulose in IMDM supplemented with 10% FCS, 1.0 U/ml human erythropoietin (Amgen), 50 ng/ml human stem cell factor (Amgen), 50 ng/ml human GM-CSF, or 10 ng/ml thrombopoietin. 500 ml of the mix was cultured either alone or on top of the adherent fibrocytes and incubated at 37°C in a humidified atmosphere of 5% CO_2 in air. All cultures were evaluated after 14 d for the presence of erythroid burst-forming units (BFU-Es) defined as an aggregate of >500 hemoglobinized cells or ≥3 erythroid subcolonies, CFU granulocyte–macrophages (CFU-GMs) defined as a cluster of >50 granulocyte and/or monocyte/macrophage cells, or CFU megakaryocytes (CFU-Megs) defined as a cluster of >10 large translucent $CD41^+$ cells.

To test whether direct contact between the fibrocytes and BM cells affected proliferation capacity, fibrocyte cultures were overlaid with 0.5% low gelling temperature agar (Sigma-Aldrich) in IMDM. After setting, the agarose was overlaid with the normal clonogenic culture media mix, and CFUs were counted as described in the previous paragraph. All experiments were performed in duplicate.

Measurement of gene expression by quantitative RT-PCR

Cultured BM-derived fibrocytes from 23 patients with PMF and 9 normal donors were examined. Fibrocytes were cultured and washed as described in the previous section. Total RNA was extracted from cultured fibrocytes by adding TRIzol reagent (Invitrogen) directly to the adherent cells. The RNA concentration was determined by NanoDrop (ND1000; Thermo Fisher Scientific), and 1 μg of total RNA was used to perform RT-PCR (SuperScript First-Strand; Invitrogen). Quantitative gene expression analysis for several target genes (Table S3) was conducted using the TaqMan expression assay kit (Applied Biosystems) or SYBR green on an ABI 7900HT FAST platform (Applied Biosystems). The Δ cycle threshold (ΔCt) value was calculated by subtracting the Ct value of a control gene (hGAP DH) from that of the target gene, and the expression level for each gene was calculated as follows: expression = $2^{-(\Delta Ct)}$.

Measurement of secreted cytokines/chemokines

Fibrocytes were cultured from BM mononuclear cells as described in the MSC culture assay and Fibrocyte cell culture assay sections. After 7 d, the supernatant was removed, the adherent cells were washed three times, and fresh fibrocyte media was added. After 10 d, the supernatants were collected for cytokine measurements. Bio-Plex prohuman inflammation 1 (37 Plex) and prohuman chemokine (40 Plex) panel assays (Bio-Rad Laboratories) were used for simultaneous quantitation of cytokines and chemokines according to the manufacturer's instructions. The samples were analyzed using the Bio-Plex system and Bio-Plex Manager software with 5PL curve fitting (Bio-Rad Laboratories). The reader was set to read a minimum of 200 beads, and the results were expressed as median fluorescence intensity. Measurement of secreted TGF-β1 and TGF-β2 was performed using the Quantikine enzyme-linked immunosorbent assay (R&D Systems).

Treatment of fibrocytes with recombinant human SAP (PRM-151) and ruxolitinib

Cultures of normal or PMF BM–derived fibrocytes were exposed to increasing concentrations of recombinant human SAP (EMD Millipore) or ruxolitinib 24 h after initiation of the cultures. The JAK1/JAK2 inhibitor ruxolitinib (Chemie Tek) was dissolved in dimethyl sulfoxide (stock solution of 5 mM) and further diluted in the culture medium. After 7 d, viable (i.e., attached to the slides and morphologically intact) fibrocytes were counted by two separate individuals. Data were normalized to the number of fibrocytes in the control (untreated) culture. The half-maximal effective concentration (EC_{50}) for SAP and ruxolitinib was calculated based on the percentage of viable fibrocytes.

Measurement of SAP, CRP, and albumin

Because SAP has been shown to inhibit fibrocyte differentiation (Pilling et al., 2003), the levels of SAP, CRP, and albumin

were measured in 10 plasma samples from healthy donors and 39 plasma samples from patients with PMF using multiplexed immunoassays (Rules-Based Medicine, Inc.), as previously described (Verstovsek et al., 2010).

BM analysis of the mouse model of MPL-W515L–induced myelofibrosis

These animal studies were performed at the Memorial Sloan Kettering Cancer Center under an animal protocol approved by the Memorial Sloan Kettering Instructional Animal Care and Utilization Committee. Female mice transplanted with BM cells expressing a mutation in the thrombopoietin receptor, MPL-W515L, developed a myelofibrosis-like phenotype characterized by thrombocytosis, splenomegaly, and reticulin fibrosis (Pikman et al., 2006). The MPL-W515L mice were generated as reported previously (Pikman et al., 2006). In brief, BM cells harvested from Balb/C mice were cultured in the presence of stem cell factor for 24 h and then infected with MPL-W515L–containing retrovirus. The infected cells were then injected into the tail veins of lethally irradiated Balb/C mice. To determine whether there is an increase in the number of fibrocytes in these mice, similar to what is seen in human PMF, we calculated the number of fibrocytes in BM and spleen samples from the MPL-W515L–transplanted mice using immunohistochemical analysis and HPF image analysis as described in the last paragraph of the Immunofluorescence section.

Xenograft mouse model

All animal studies were performed at the MD Anderson Cancer Center under an animal protocol approved by the MD Anderson Cancer Center Instructional Animal Care and Utilization Committee. To establish the xenograft mouse model, PMF BM–derived low-density cells (10^6 suspended in 100 µl IMDM) were injected into the tail vein of ten 4–6-wk-old female NSG mice homozygous for *Prkdc*^{scid} and *IL-2Rg*^{tm1Wjl} (The Jackson Laboratory). As a control, 10 mice were also injected with normal BM low-density cells, and 10 mice were injected with IMDM. Engraftment of human cells was assessed 2 wk after injection and once a month thereafter by flow cytometry of PB cells using FITC-labeled anti–HLA-ABC antibodies (BD) and by RT-PCR to measure the *JAK2* allele burden. We obtained the same level of engraftment in lethally irradiated and unirradiated mice. Therefore, to circumvent any radiation-induced abnormalities, we performed all transplant experiments in unirradiated mice.

Assessment of SAP (PRM-151) treatment

In our initial xenograft mouse model experiments, we used 10 mice per group, and all mice in the placebo group died, whereas none in the SAP treatment group died. If we assume a survival rate of 10% for mice in the placebo group and 90% for those in the treatment groups, using 10 mice per group gives us a power of 82% with a type I error rate of 0.05%.

NSG mice transplanted with PMF BM–derived cells were randomized into four groups of 10 mice as follows: (1) injected intravenously with IMDM but no BM cells, (2) transplanted with PMF BM cells and treated with placebo, (3) transplanted and treated with 10 mg/kg recombinant human SAP (PRM-151; Promedior, Inc.) starting 2 wk after transplantation, and (4) transplanted and treated with 10 mg/kg SAP starting 2 mo after transplantation. The treated mice were given PRM-151 intraperitoneally daily for 9 d and on two consecutive days weekly thereafter. This treatment schedule was used to mimic a human dosing schedule of days 1, 3, and 5 and then once a week, based on the knowledge that the half-life of PRM-151 in mice is much shorter than that in humans ($t_{1/2}$ = 8 vs. 30 h, respectively). Animals were selected at random by cage number for each treatment group before the injection of BM cells.

We also tested the effects of SAP in MPL-W515L mice. SAP treatment was started the day after induction following the treatment schedule described above (Fig. 9 A). The mice were euthanized in accordance with the experimental protocol when they became moribund, were unable to obtain food or water, or if they lost ≥20% of their body weight. Immediately after euthanasia, mouse femurs were removed and flushed with IMDM to extract BM cells for use in quantitative PCR and FISH analyses as described in the sections describing FISH and quantitation of gene mutations.

Cytogenetic analysis

Immediately after euthanasia, mouse femurs were removed and flushed with IMDM, and the flushed BM cells were washed twice and cultured in 20% FBS/IMDM supplemented with 100 U/ml penicillin and 100 µg/ml streptomycin for 4 h at 37°C. The cultured cells were incubated with 0.075 M KCl at room temperature for 20 min, after which 3 ml of a 3:1 methanol/acetic acid (vol/vol) was added. Cells were then washed three times and dropped onto a wet glass slide and air dried. Slides were optimally aged (3 d at 65°C), and then Giemsa was banded following routine laboratory techniques. G-band metaphase spreads from each sample were photographed using a microscope (80i; Nikon) equipped with karyotyping software from Applied Spectral Imaging Inc.

Morphological analysis

Morphological analysis of mouse tissue was conducted after staining tissues with hematoxylin and eosin (H&E) using standard methods. For the assessment of reticulin fibrosis, tissues were silver stained using a standard method. An expert pathologist (C.E. Bueso-Ramos) performed the morphological analysis and interpretation. All histological and morphological comparisons of BM histology, fibrocyte morphology, and silver staining were assessed in a blinded fashion by a hematopathologist who was not aware of the project, its details, or the significance of the findings on the slides he analyzed. The degree of BM fibrosis was assessed according to the European consensus criteria (Thiele et al., 2005).

Statistical analysis

Groups were compared using two-sided Student's *t* tests with Welch's correction in cases where the variances were not equal. Differential gene expression or cytokine levels were visualized as heat maps using the Java TreeView extensible visualization of microarray data. The Kaplan-Meier method was used to analyze overall survival of mice. The log-rank test was used to compare survival. Linear correlations were measured with the Pearson correlation coefficient. All statistical analyses were performed using Prism software (v6; GraphPad Software).

Online supplemental material

Table S1 shows baseline characteristics of the patients. Table S2 shows antibodies and FISH probes used in immunofluorescent analysis. Table S3 shows target genes and primers used in RT-PCR. Table S4 shows the percentage of human HLA-ABC$^+$ cells in xenograft mice over their lifetime. Online supplemental material is available at http://www.jem.org/cgi/content/full/jem.20160283/DC1.

ACKNOWLEDGMENTS

This research was performed in part in the Flow Cytometry and Cellular Imaging and Molecular Cytogenetics Core Facility, Center for Genetics and Genomics, which is supported in part by the MD Anderson Cancer Center support grant CA016672. The authors thank the family of Hanns A. Pielenz for their generous donation supporting this research.

D. Pilling has equity in Promedior, Inc. The authors declare no additional competing financial interests.

Author contributions: S. Verstovsek directed the project, obtained patient samples, and analyzed data. T. Manshouri designed and carried out experiments, analyzed data, and wrote the manuscript. D. Pilling, L. Knez, S.M. Post, C.E. Bueso-Ramos, E.L. Spaeth, D.M. Harris, and C.J. Creighton carried out experiments and analyzed data. K.J. Newberry analyzed the data and wrote the manuscript. H.M. Kantarjian provided patient samples and analyzed the clinical data. R.L. Levine provided tissue from MPL-W515L mice and reviewed the manuscript. C.J. Creighton performed statistical analyses. Z. Estrov designed and directed the project, analyzed data, and wrote the manuscript. All authors reviewed the final manuscript.

Submitted: 22 February 2016
Accepted: 22 June 2016

REFERENCES

Abe, R., S.C. Donnelly, T. Peng, R. Bucala, and C.N. Metz. 2001. Peripheral blood fibrocytes: differentiation pathway and migration to wound sites. *J. Immunol.* 166:7556–7562. http://dx.doi.org/10.4049/jimmunol.166.12.7556

Arranz, L., A. Sánchez-Aguilera, D. Martín-Pérez, J. Isern, X. Langa, A. Tzankov, P. Lundberg, S. Muntión, Y.S. Tzeng, D.M. Lai, et al. 2014. Neuropathy of haematopoietic stem cell niche is essential for myeloproliferative neoplasms. *Nature.* 512:78–81.

Bhatia, M., D. Bonnet, B. Murdoch, O.I. Gan, and J.E. Dick. 1998. A newly discovered class of human hematopoietic cells with SCID-repopulating activity. *Nat. Med.* 4:1038–1045. http://dx.doi.org/10.1038/2023

Bottazzi, B., A. Doni, C. Garlanda, and A. Mantovani. 2010. An integrated view of humoral innate immunity: pentraxins as a paradigm. *Annu. Rev. Immunol.* 28:157–183. http://dx.doi.org/10.1146/annurev-immunol-030409-101305

Bucala, R., L.A. Spiegel, J. Chesney, M. Hogan, and A. Cerami. 1994. Circulating fibrocytes define a new leukocyte subpopulation that mediates tissue repair. *Mol. Med.* 1:71–81.

Castaño, A.P., S.L. Lin, T. Surowy, B.T. Nowlin, S.A. Turlapati, T. Patel, A. Singh, S. Li, M.L. Lupher Jr., and J.S. Duffield. 2009. Serum amyloid P inhibits fibrosis through FcγR-dependent monocyte-macrophage regulation in vivo. *Sci. Transl. Med.* 1:5ra13. http://dx.doi.org/10.1126/scitranslmed.3000111

Castro-Malaspina, H., R.E. Gay, S.C. Jhanwar, J.A. Hamilton, D.R. Chiarieri, P.A. Meyers, S. Gay, and M.A. Moore. 1982. Characteristics of bone marrow fibroblast colony-forming cells (CFU-F) and their progeny in patients with myeloproliferative disorders. *Blood.* 59:1046–1054.

Cox, N., D. Pilling, and R.H. Gomer. 2015. DC-SIGN activation mediates the differential effects of SAP and CRP on the innate immune system and inhibits fibrosis in mice. *Proc. Natl. Acad. Sci. USA.* 112:8385–8390. http://dx.doi.org/10.1073/pnas.1500956112

Estrov, Z., A. Tawa, X.H. Wang, I.D. Dubé, H. Sulh, A. Cohen, E.W. Gelfand, and M.H. Freedman. 1987. In vitro and in vivo effects of deferoxamine in neonatal acute leukemia. *Blood.* 69:757–761.

Greenberg, B.R., L. Woo, I.C. Veomett, C.M. Payne, and F.R. Ahmann. 1987. Cytogenetics of bone marrow fibroblastic cells in idiopathic chronic myelofibrosis. *Br. J. Haematol.* 66:487–490. http://dx.doi.org/10.1111/j.1365-2141.1987.tb01332.x

Groopman, J.E. 1980. The pathogenesis of myelofibrosis in myeloproliferative disorders. *Ann. Intern. Med.* 92:857–858. http://dx.doi.org/10.7326/0003-4819-92-6-857

Harrison, C., J.J. Kiladjian, H.K. Al-Ali, H. Gisslinger, R. Waltzman, V. Stalbovskaya, M. McQuitty, D.S. Hunter, R. Levy, L. Knoops, et al. 2012. JAK inhibition with ruxolitinib versus best available therapy for myelofibrosis. *N. Engl. J. Med.* 366:787–798. http://dx.doi.org/10.1056/NEJMoa1110556

Haudek, S.B., Y. Xia, P. Huebener, J.M. Lee, S. Carlson, J.R. Crawford, D. Pilling, R.H. Gomer, J. Trial, N.G. Frangogiannis, and M.L. Entman. 2006. Bone marrow-derived fibroblast precursors mediate ischemic cardiomyopathy in mice. *Proc. Natl. Acad. Sci. USA.* 103:18284–18289. http://dx.doi.org/10.1073/pnas.0608799103

Haudek, S.B., J. Trial, Y. Xia, D. Gupta, D. Pilling, and M.L. Entman. 2008. Fc receptor engagement mediates differentiation of cardiac fibroblast precursor cells. *Proc. Natl. Acad. Sci. USA.* 105:10179–10184. http://dx.doi.org/10.1073/pnas.0804910105

Hong, K.M., J.A. Belperio, M.P. Keane, M.D. Burdick, and R.M. Strieter. 2007. Differentiation of human circulating fibrocytes as mediated by transforming growth factor-β and peroxisome proliferator-activated receptor γ. *J. Biol. Chem.* 282:22910–22920. http://dx.doi.org/10.1074/jbc.M703597200

Hutchinson, W.L., E. Hohenester, and M.B. Pepys. 2000. Human serum amyloid P component is a single uncomplexed pentamer in whole serum. *Mol. Med.* 6:482–493.

International Agency for Research on Cancer and World Health Organization. Swerdlow, S.H., E. Campo, N.L. Harris, E.S. Jaffe, S.A. Pileri, H. Stein, J. Thiele, and J.W. Vardiman, editors. 2008. WHO classification of tumours of haematopoietic and lymphoid tissues. World Health Organization Press, Lyon, France. 439 pp.

Jacobson, R.J., A. Salo, and P.J. Fialkow. 1978. Agnogenic myeloid metaplasia: a clonal proliferation of hematopoietic stem cells with secondary myelofibrosis. *Blood.* 51:189–194.

Keeley, E.C., B. Mehrad, and R.M. Strieter. 2011. The role of fibrocytes in fibrotic diseases of the lungs and heart. *Fibrogenesis Tissue Repair.* 4:2. http://dx.doi.org/10.1186/1755-1536-4-2

Kisseleva, T., H. Uchinami, N. Feirt, O. Quintana-Bustamante, J.C. Segovia, R.F. Schwabe, and D.A. Brenner. 2006. Bone marrow-derived fibrocytes

participate in pathogenesis of liver fibrosis. *J. Hepatol.* 45:429–438. http://dx.doi.org/10.1016/j.jhep.2006.04.014

Klampfl, T., H. Gisslinger, A.S. Harutyunyan, H. Nivarthi, E. Rumi, J.D. Milosevic, N.C.C. Them, T. Berg, B. Gisslinger, D. Pietra, et al. 2013. Somatic mutations of calreticulin in myeloproliferative neoplasms. *N. Engl. J. Med.* 369:2379–2390. http://dx.doi.org/10.1056/NEJMoa1311347

Kleaveland, K.R., B.B. Moore, and K.K. Kim. 2014. Paracrine functions of fibrocytes to promote lung fibrosis. *Expert Rev. Respir. Med.* 8:163–172. http://dx.doi.org/10.1586/17476348.2014.862154

Maharjan, A.S., D. Pilling, and R.H. Gomer. 2011. High and low molecular weight hyaluronic acid differentially regulate human fibrocyte differentiation. *PLoS One.* 6:e26078. http://dx.doi.org/10.1371/journal.pone.0026078

Martyré, M.C., M.C. Le Bousse-Kerdiles, N. Romquin, S. Chevillard, V. Praloran, J.L. Demory, and B. Dupriez. 1997. Elevated levels of basic fibroblast growth factor in megakaryocytes and platelets from patients with idiopathic myelofibrosis. *Br. J. Haematol.* 97:441–448. http://dx.doi.org/10.1046/j.1365-2141.1997.292671.x

Mehrad, B., and R.M. Strieter. 2012. Fibrocytes and the pathogenesis of diffuse parenchymal lung disease. *Fibrogenesis Tissue Repair.* 5:S22. http://dx.doi.org/10.1186/1755-1536-5-S1-S22

Murray, L.A., Q. Chen, M.S. Kramer, D.P. Hesson, R.L. Argentieri, X. Peng, M. Gulati, R.J. Homer, T. Russell, N. van Rooijen, et al. 2011. TGF-beta driven lung fibrosis is macrophage dependent and blocked by Serum amyloid P. *Int. J. Biochem. Cell Biol.* 43:154–162. http://dx.doi.org/10.1016/j.biocel.2010.10.013

Nowell, P.C., and J.B. Finan. 1978. Cytogenetics of acute and chronic myelofibrosis. *Virchows Arch. B Cell Pathol. Incl. Mol. Pathol.* 29:45–50.

Ohishi, M., W. Ono, N. Ono, R. Khatri, M. Marzia, E.K. Baker, S.H. Root, T.L. Wilson, Y. Iwamoto, H.M. Kronenberg, et al. 2012. A novel population of cells expressing both hematopoietic and mesenchymal markers is present in the normal adult bone marrow and is augmented in a murine model of marrow fibrosis. *Am. J. Pathol.* 180:811–818. http://dx.doi.org/10.1016/j.ajpath.2011.10.028

Pikman, Y., B.H. Lee, T. Mercher, E. McDowell, B.L. Ebert, M. Gozo, A. Cuker, G. Wernig, S. Moore, I. Galinsky, et al. 2006. MPLW515L is a novel somatic activating mutation in myelofibrosis with myeloid metaplasia. *PLoS Med.* 3:e270. http://dx.doi.org/10.1371/journal.pmed.0030270

Pilling, D., C.D. Buckley, M. Salmon, and R.H. Gomer. 2003. Inhibition of fibrocyte differentiation by serum amyloid P. *J. Immunol.* 171:5537–5546. http://dx.doi.org/10.4049/jimmunol.171.10.5537

Pilling, D., D. Roife, M. Wang, S.D. Ronkainen, J.R. Crawford, E.L. Travis, and R.H. Gomer. 2007. Reduction of bleomycin-induced pulmonary fibrosis by serum amyloid P. *J. Immunol.* 179:4035–4044. http://dx.doi.org/10.4049/jimmunol.179.6.4035

Pilling, D., T. Fan, D. Huang, B. Kaul, and R.H. Gomer. 2009. Identification of markers that distinguish monocyte-derived fibrocytes from monocytes, macrophages, and fibroblasts. *PLoS One.* 4:e7475. http://dx.doi.org/10.1371/journal.pone.0007475

Quintás-Cardama, A., T. Manshouri, Z. Estrov, D. Harris, Y. Zhang, A. Gaikwad, H.M. Kantarjian, and S. Verstovsek. 2011. Preclinical characterization of atiprimod, a novel JAK2 AND JAK3 inhibitor. *Invest. New Drugs.* 29:818–826. http://dx.doi.org/10.1007/s10637-010-9429-z

Rampal, R., F. Al-Shahrour, O. Abdel-Wahab, J.P. Patel, J.P. Brunel, C.H. Mermel, A.J. Bass, J. Pretz, J. Ahn, T. Hricik, et al. 2014. Integrated genomic analysis illustrates the central role of JAK-STAT pathway activation in myeloproliferative neoplasm pathogenesis. *Blood.* 123:e123–e133. http://dx.doi.org/10.1182/blood-2014-02-554634

Reich, B., K. Schmidbauer, M. Rodriguez Gomez, F. Johannes Hermann, N. Göbel, H. Brühl, I. Ketelsen, Y. Talke, and M. Mack. 2013. Fibrocytes develop outside the kidney but contribute to renal fibrosis in a mouse model. *Kidney Int.* 84:78–89. http://dx.doi.org/10.1038/ki.2013.84

Reilkoff, R.A., R. Bucala, and E.L. Herzog. 2011. Fibrocytes: emerging effector cells in chronic inflammation. *Nat. Rev. Immunol.* 11:427–435. http://dx.doi.org/10.1038/nri2990

Steel, D.M., and A.S. Whitehead. 1994. The major acute phase reactants: C-reactive protein, serum amyloid P component and serum amyloid A protein. *Immunol. Today.* 15:81–88. http://dx.doi.org/10.1016/0167-5699(94)90138-4

Thiele, J., and H.M. Kvasnicka. 2006. Grade of bone marrow fibrosis is associated with relevant hematological findings-a clinicopathological study on 865 patients with chronic idiopathic myelofibrosis. *Ann. Hematol.* 85:226–232. http://dx.doi.org/10.1007/s00277-005-0042-8

Thiele, J., H.M. Kvasnicka, F. Facchetti, V. Franco, J. van der Walt, and A. Orazi. 2005. European consensus on grading bone marrow fibrosis and assessment of cellularity. *Haematologica.* 90:1128–1132.

Tiedt, R., H. Hao-Shen, M.A. Sobas, R. Looser, S. Dirnhofer, J. Schwaller, and R.C. Skoda. 2008. Ratio of mutant JAK2-V617F to wild-type Jak2 determines the MPD phenotypes in transgenic mice. *Blood.* 111:3931–3940. http://dx.doi.org/10.1182/blood-2007-08-107748

Triviai, I., M. Ziegler, U. Bergholz, A.J. Oler, T. Stübig, V. Prassolov, B. Fehse, C.A. Kozak, N. Kröger, and C. Stocking. 2014. Endogenous retrovirus induces leukemia in a xenograft mouse model for primary myelofibrosis. *Proc. Natl. Acad. Sci. USA.* 111:8595–8600. http://dx.doi.org/10.1073/pnas.1401215111

van Dop, W.A., J. Heijmans, N.V. Büller, S.A. Snoek, S.L. Rosekrans, E.A. Wassenberg, M.A. van den Bergh Weerman, B. Lanske, A.R. Clarke, D.J. Winton, et al. 2010. Loss of Indian Hedgehog activates multiple aspects of a wound healing response in the mouse intestine. *Gastroenterology.* 139:1665–1676.e10. http://dx.doi.org/10.1053/j.gastro.2010.07.045

Vener, C., N.S. Fracchiolla, U. Gianelli, R. Calori, F. Radaelli, A. Iurlo, S. Caberlon, G. Gerli, L. Boiocchi, and G.L. Deliliers. 2008. Prognostic implications of the European consensus for grading of bone marrow fibrosis in chronic idiopathic myelofibrosis. *Blood.* 111:1862–1865. http://dx.doi.org/10.1182/blood-2007-09-112953

Verstegen, M.M., J.J. Cornelissen, W. Terpstra, G. Wagemaker, and A.W. Wognum. 1999. Multilineage outgrowth of both malignant and normal hemopoietic progenitor cells from individual chronic myeloid leukemia patients in immunodeficient mice. *Leukemia.* 13:618–628. http://dx.doi.org/10.1038/sj.leu.2401366

Verstovsek, S., H. Kantarjian, R.A. Mesa, A.D. Pardanani, J. Cortes-Franco, D.A. Thomas, Z. Estrov, J.S. Fridman, E.C. Bradley, S. Erickson-Viitanen, et al. 2010. Safety and efficacy of INCB018424, a JAK1 and JAK2 inhibitor, in myelofibrosis. *N. Engl. J. Med.* 363:1117–1127. http://dx.doi.org/10.1056/NEJMoa1002028

Verstovsek, S., R.A. Mesa, J. Gotlib, R.S. Levy, V. Gupta, J.F. DiPersio, J.V. Catalano, M. Deininger, C. Miller, R.T. Silver, et al. 2012. A double-blind, placebo-controlled trial of ruxolitinib for myelofibrosis. *N. Engl. J. Med.* 366:799–807. http://dx.doi.org/10.1056/NEJMoa1110557

Wang, J.C., H.D. Lang, S. Lichter, M. Weinstein, and P. Benn. 1992. Cytogenetic studies of bone marrow fibroblasts cultured from patients with myelofibrosis and myeloid metaplasia. *Br. J. Haematol.* 80:184–188. http://dx.doi.org/10.1111/j.1365-2141.1992.tb08898.x

Yang, L., P.G. Scott, J. Giuffre, H.A. Shankowsky, A. Ghahary, and E.E. Tredget. 2002. Peripheral blood fibrocytes from burn patients: identification and quantification of fibrocytes in adherent cells cultured from peripheral blood mononuclear cells. *Lab. Invest.* 82:1183–1192. http://dx.doi.org/10.1097/01.LAB.0000027841.50269.61

Zanjani, E.D., G. Almeida-Porada, A.G. Livingston, A.W. Flake, and M. Ogawa. 1998. Human bone marrow CD34- cells engraft in vivo and undergo multilineage expression that includes giving rise to CD34+ cells. *Exp. Hematol.* 26:353–360.

Zhang, H., I. Maric, M.J. DiPrima, J. Khan, R.J. Orentas, R.N. Kaplan, and C.L. Mackall. 2013. Fibrocytes represent a novel MDSC subset circulating in patients with metastatic cancer. *Blood.* 122:1105–1113. http://dx.doi.org/10.1182/blood-2012-08-449413